# Dryland endolithic Chroococcidiopsis and temperate fresh water Synechocystis have distinct membrane lipid and photosynthesis acclimation strategies upon desiccation and temperature increase

Damien Douchi, Gregory Si Larbi, Benjamin Fel, Marlène Bonnanfant,
Mathilde Louwagie, Juliette Jouhet, Mathias Agnely, Stéphanie Pouget, Eric
Maréchal

**HAL Id: hal-04281075**

**https://hal.science/hal-04281075**

Submitted on 12 Nov 2023

**Title**

Dryland endolithic *Chroococcidiopsis* and temperate fresh water *Synechocystis* have distinct membrane lipid and photosynthesis acclimation strategies upon desiccation and temperature increase

**Authors**

Damien Douchi[1], Gregory Si Larbi[1], Benjamin Fel[1], Marlène Bonnanfant[1,$], Mathilde Louwagie[1], Juliette Jouhet[1], Mathias Agnely[2], Stéphanie Pouget[3], Eric Maréchal[1,*]

**Affiliations**

[1]Laboratoire de Physiologie Cellulaire et Végétale, Commissariat à l'Energie Atomique et aux Energies Alternatives, Institut National de Recherche pour l'Agriculture, l'Alimentation et l'Environnement, Centre National de la Recherche Scientifique, Université Grenoble Alpes; IRIG, CEA-Grenoble, 17 rue des Martyrs; 38000 Grenoble, France

[2]SAINT-GOBAIN RESEARCH PARIS, 39 quai Lucien Lefranc, 93303 Aubervilliers Cedex France

[3]Laboratoire Modélisation et Exploration des Matériaux; Université Grenoble Alpes, Commissariat à l'énergie atomique et aux énergies alternatives; IRIG; CEA-Grenoble, 17 rue des Martyrs, 38000 Grenoble, France

[$]Present adress: Centre d'Étude et de Valorisation des Algues, 83 Rue de Pen Lan, 22610 Pleubian, France

*correspondence: Eric Maréchal, eric.marechal@cea.fr

**Running title**

Cyanobacteria acclimation to climate change

**Plant & Cell Physiology subject area.**

- environmental and stress responses
- Special Issue on "Plant and Algal Lipids: In All Their States and On All Scales"

**Keywords**

*Synechocystis*, *Chroococcidiopsis*, endolithic cyanobacteria, sulfoquinovosyldiacylglycerol, gypsum, photosynthesis

**Abstract.**

An effect of climate change is the expansion of drylands in temperate regions, predicted to affect microbial biodiversity. Photosynthetic organisms being at the base of ecosystem's trophic networks, we compared an endolithic desiccation-tolerant *Chroococcidiopsis* cyanobacteria isolated from gypsum rocks in the Atacama Desert, with a freshwater desiccation-sensitive *Synechocystis*. We sought whether some acclimation traits in response to desiccation and temperature variations were shared, to evaluate the potential of temperate species to possibly become resilient to future arid conditions. When temperature varies, *Synechocystis* tunes the acyl composition of its lipids, via a homeoviscuous acclimation mechanism known to adjust membrane fluidity, whereas no such change occurs in *Chroococcidiopsis*. *Vice versa*, a combined study of photosynthesis and pigment content shows that *Chroococcidiopsis* remodels its photosynthesis components and keeps an optimal photosynthetic capacity at all temperatures, whereas *Synechocystis* is unable to such adjustment. Upon desiccation on a gypsum surface, *Synechocystis* is rapidly unable to revive, whereas *Chroococcidiopsis* is capable to recover after three weeks. Using X-ray diffraction, we found no evidence that *Chroococcidiopsis* could use water extracted from gypsum crystal in such conditions, as a surrogate of missing water. The sulfolipid sulfoquinovosyldiacylglycerol becomes the prominent membrane lipid in both dehydrated cyanobacteria, highlighting an overlooked function for this lipid. *Chroococcidiopsis* keeps a minimal level of monogalactosyldiacylglycerol, which may be essential for the recovery process. Results support that two independent adaptation strategies have evolved in these species to cope with temperature and desiccation increase, and suggest some possible scenarios for microbial biodiversity change triggered by climate change.

**Introduction**

The impact of climate change is marked by a global expansion of drylands, expected to lead to dramatic changes in the structure and composition of microbial biodiversity in a multitude of aero-terrestrial habitats. In these regions, a shift is predicted to occur, towards mechanisms prevalent in currently dry regions, referred to as 'dryland mechanisms' (Grunzweig et al. 2022). Whereas these ecosystems will evolve by the adaptation of local species, the colonization by external organisms, or a combination of both is an open question. Photosynthetic organisms are at the base of ecosystem's trophic networks, and most known species are not resilient enough to overcome anticipated longer arid and warm periods leading to the formation of deserts. Species populating extent arid zones may be pioneers in these expanding areas, but our understanding of the fundamental mechanisms that allow their development in an extremely dry environment is still poor. Their capacity to colonize novel areas is unknown.

Cyanobacteria from the *Chroococcidiopsis* genus thrive in hot and cold deserts, from equatorial to Arctic and Antarctic regions (Bahl et al. 2011; Lacap-Bugler et al. 2017). Their abundance increases with declining water availability (Hagemann et al. 2015). They are known to resist to harsh conditions such as short-wavelength UV (Baque et al. 2013) or ionizing radiations (Billi et al. 2000; Verseux et al. 2017), and extremely high salinity (Casero et al. 2021). However, *Chroococcidiopsis* are very sensitive to high light intensity (Casero et al. 2021) and their defense relies on an avoidance strategy, by spreading a few millimeters under the surface of translucent rocks, where just 0.1–2.5% of the total incident solar radiation might reach them (Casero et al. 2021; Wierzchos et al. 2018). Endolithic *Chroococcidiopsis* are then primary producers at the base of a trophic network for microbial communities, including bacteria and fungi (Coleine et al. 2021; Gomez-Silva et al. 2019; Walker and Pace 2007).

*Chroococcidiopsis* can colonize a multitude of endolithic habitats, from quartz ($SiO_2$) containing rocks such as sandstone (Gomez-Silva 2018; Murray et al. 2022) or ignimbrite (Camara et al. 2014), to calcite ($CaCO_3$) (Casero et al. 2021; Murray et al. 2022) or gypsum ($Ca(SO_4)(H_2O)_2$) (Murray et al. 2022). In the latter case, it was suggested that *Chroococcidiopsis* could maintain photosynthetic activity beyond periods without moisture, by extracting the $H_2O$ molecules of the crystalline structure, converting gypsum into anhydrite ($CaSO_4$) (Huang et al. 2020), but the validity of the experiments performed and their interpretation have been contested, both in practical and theoretical terms (Wierzchos et al. 2020).

The adaptation mechanisms allowing *Chroococcidiopsis* to live in very dry environments in cold or hot deserts, exposed to important daily variations of temperature, are therefore still puzzling. The role played by membrane glycerolipids has not yet been studied. Membrane glycerolipids are formed by a three-carbon glycerol backbone (numbered *sn*-1, *sn*-2 and *sn*-3), harboring a polar head group at position *sn*-3, and acyl chains at positions *sn*-1 and *sn*-2. The polar head group defines the lipid class: five are conserved in cyanobacteria, including four glycolipids, *i.e.* monoglucosyl-, monogalactosyl-, digalactosyl- and sulfoquinovosyl-diacylglycerol (MGlcDG, MGDG, DGDG and SQDG, respectively) and one phospholipid, *i.e.* phosphatidylglycerol (PG). Acyl groups have various chain-lengths, ranging usually from 14 to 18 carbons, and they can contain double bonds, or unsaturations, introduced irreversibly by enzymes called desaturases. In other cyanobacteria such as *Demonostoc salinum*, living in saline lakes, highly unsaturated lipids were suggested to contribute to the resistance to desiccation (de Alvarenga et al. 2020). Likewise, in marine *Synechococcus*, chain-length and saturation level of membrane glycerolipids was determinant in thermoacclimation in warm or cold oceanic regions, with an increase of acyl unsaturation and shortening of chain length, when temperature decreased (Pittera et al. 2018).

Here, we used *Chroococcidiopsis* G-MTQ-3P2 (hereafter *Chroococcidiopsis*), isolated from the Atacama desert and previously reported to be able to extract $H_2O$ from gypsum upon long exposures of dryness (Huang et al. 2020). We reevaluated this property. We then determined the complete glycerolipidome of this cyanobacteria strain and analyzed lipidomic changes upon exposure to increasing temperature and long periods of desiccation, in comparison with *Synechocystis* sp. PCC 6803 (hereafter *Synechocystis*), a desiccation- and temperature-sensitive cyanobacterium. We then analyzed cell ultrastructure and photosynthetic features in response to dryness and temperature.

**Results**

**Incubation of *Chroococcidiopsis* G-MTQ-3P2 and *Synechocystis* PCC 6803 at the surface of gypsum, in desiccation conditions does not support a capacity to extract crystalline $H_2O$**

We reexamined the capacity of *Chroococcidiopsis* G-MTQ-3P2 to extract $H_2O$ from gypsum reported recently (Huang et al. 2020). In this study, *Chroococcidiopsis* was suggested to form a 'biofilm' at the rock surface. X Ray diffraction (XRD) was used to assess that a phase transition occurred in gypsum exposed to *Chroococcidiopsis* when no water was provided, leading to the detection of anhydrite, indicating a removal of $H_2O$ from the crystal structure (Huang et al. 2020). We used pure chips of gypsum, with a larger surface (176 $mm^2$) as that previously used (40 $mm^2$) to limit dehydration due to dimension or edge effects. We deposited freshly grown cyanobacteria to the surface of the chips, with a quantity normalized on initial chlorophyll content (3 μg chlorophyll per chip, final). The porosity of the polycrystalline chips allowed the initial retention of water and nutrients from the 100-μL volume of medium accompanying the cyanobacterial inoculated. We then incubated chips for at least 15 days, at 25°C under constant light, as described in past studies. All treatments were performed in triplicates, with series of chips collected at Day 0 to 15 for XRD analyses. Whereas chips covered with *Chroococcidiopsis* darkened and turned brownish showing a pigment reorganisation, those covered with *Synechocystis* highlighted a decrease of chlorophyll, leaving the blue pigment phycocyanin mostly visible (Fig. 1A), suggesting an impairment of cell integrity and oxidation and bleaching of chlorophyll pigments in this desiccation-sensitive control cyanobacterium.

After incubation, the mineral composition of chips was measured in a Panalytical Empyrean XRD using a Cobalt source and compared to a control chip only inoculated with 100 μL of sterile BG11 medium (blank). XRD analyses performed on each chip of a triplicate treatment, showed no variation between samples (Fig. 1B). Considering the expected patterns for gypsum and the low-hydrated calcium sulfate forms bassanite and anhydrite (further confirmed by the measurement of the diffraction patterns of control samples of bassanite, β-anhydrite and γ-anhydrite), it can be concluded, from the presence of a strong diffraction peak at 11.6° and the absence of peak close to 14.6° and 25.4°, that only the $Ca(SO_4)(H_2O)_2$ gypsum phase is present, even after 15 days. This time point was selected as the biomass had been dried for several days, and no further change in the substrate was expected beyond that point. No difference could be observed between any of the chips exposed to *Chroococcidiopsis* or *Synechocystis* and an untreated gypsum control (Fig. 1C).

Figure 1

In the initial study, biological dehydration was investigated on gypsum single crystals (Huang et al. 2020). More specifically, $H_2O$ removal was reported to be anisotropic and favored by depositing cyanobacteria on the (011) faces of the crystal. We therefore pursued our attempts using gypsum single crystals with large (011) faces. A crystal obtained from a gypsum quarry was confirmed to be monocrystalline by Laue XRD. We cut centimetric sized pieces presenting (011) surface, as well as (010) surface pieces used as a control. These single crystal pieces were subjected to the same incubation, with 100 μL BG11 medium for the blank and 100 μL corresponding to 20 μg chlorophyll *Chroococcidipsis* and *Synechocystis*, deposited on (011) or (010) faces. After a 30-day incubation, the gypsum pieces were analyzed by X-ray diffraction (Supplemental Fig. S1). The peak close to 33.4° results from X-ray diffraction by (011) planes of pure gypsum, while those close to 11.6° and 23.4° are associated to (010) planes, confirming the correct orientation of the surface cuts (Supplemental Fig. S1A and B, Blank). The comparison between the *Synechocystis* and *Chroococcidiopsis* strains to the blank revealed no significant difference in both surface orientations indicating the absence of gypsum dehydration (Supplemental Fig. S1A and B).

We have taken the characterization a step further by scrapping off the first few μm at the (011) surface of each crystal considering the possibility that the dehydration could be local and minor in the volume of gypsum probed by the X-ray beam. Supplemental Fig. S1C displays the diffractograms obtained with the scrapped samples. The comparison of the extract from the cultivated oriented (011) gypsum pieces revealed no significant difference between the blank, and crystals treated in the presence of *Synechocystis* or *Chroococcidiopsis*. The presence of a diffraction peak at 11.6° and the absence of any peak close to 14.6° and 25.4° indicates again that only the $Ca(SO_4)(H_2O)_2$ gypsum phase is present, refuting any dehydration activity in the tested conditions

We wondered whether the absence of dehydration of gypsum was due to a loss of cell integrity of cyanobacteria in the course of the experiment. We transferred polycrystalline chips treated 0, 2 and 15 days in a fresh liquid BG11 medium, and measured whether cells could still grow following treatment. After 15 days without any provision of water, *Synechocystis* cells were completely dead, whereas part of *Chroococcidiospsis* cells could recover, after a lag period of about four days (Fig. 2).

Figure 2

We addressed the impact of dehydration on the surface of gypsum chips on photosynthesis efficiency. In both *Chroococcidiospsis* and *Synechocystis*, incubation at the surface of gypsum chips in dehydrated conditions led to a decrease of Fv/Fm. However, after three weeks, whereas no photosynthesis could be measured in *Synechocystis*, *Chroococcidiospsis* cells highlighted a weak but stable level, indicating its resilience to very long periods of dehydration (Fig 3A).

Figure 3

Thus, although *Chroococcidiospsis* G-MTQ-3P2 inoculum remained, at least partly, alive in the course of the incubation without any external addition of water, no extraction of $H_2O$ from the crystal structure of gypsum could be observed, and we could not confirm past results on this supposed property. In this experimental system, *Chroococcidiospsis* proved to be remarkably resistant to long periods of desiccation.

**Ultrastructure of cyanobacteria following desiccation on gypsum reveals the preservation of thylakoid structure in *Chroococcidiopsis***

Since desiccation treatments on the surface of gypsum led to a strong effect on photosynthesis and capacity to recover and grow, we addressed the impact on cyanobacteria cell ultrastructure by scanning transmission electronic microscopy (STEM) (Fig. 4). *Synechocystis* was used as a control (Fig. 4A and B)

Figure 4

The ultrastructure of *Synechocystis* and *Chroococcidiopsis* in liquid culture (Fig. 4A and C) was consistent with previous descriptions (Billi et al. 2001; Casero et al. 2021; Sobotka et al. 2008). The cell wall is thicker in *Chroococcidiopsis* compared to *Synechocystis* in both liquid condition and following three weeks of desiccation (Fig. 4C and D). This feature is considered essential in the resistance to dehydration, limiting water permeability and losses. In highly dehydrated conditions, we also observed the development of an extracellular matrix (Fig. 4D, top right corner) around the *Chroococcidiopsis* cells, possibly playing a role in *Chroococcidiopsis* interactions with its substrate. Additionally the cell wall contains scytonemin, a UV absorbing compound extremely potent in protecting the cell against UV damages (Casero et al. 2021).

The thylakoid membrane architecture appears very different in both species. Thylakoids appear more irregular and wavy in *Chroococcidiopsis*, as reported earlier (Billi et al. 2001; Casero et al. 2021). The thylakoids of *Synechocystis* are organized in membrane pairs (van de Meene et al. 2006), which contrasts with the electron dense single layer thylakoids observed in *Chroococcidiopsis* (Fig. 4A and C, arrows).

The dry stage of *Synechocystis* and *Chroococcodiopsis* showed the appearance of granules in the cytoplasm (Fig. 4B and D), reminiscent of the glycogen reserves and the PHB or Poly-P structures of cyanothece, respectively (Schneegurt et al. 1994; Welkie et al. 2013). The biochemical characterization of these structures needs future analyses; however they suggest the formation of storage forms in response to desiccation.

Eventually, whereas thylakoid architecture appeared dismantled in dried *Synechocystis* cells (Fig. 4, arrows), photosynthetic membranes seemed less affected after dehydration of *Chroococcidiopsis* (Fig. 4D). We therefore addressed whether lipid membrane composition and photosynthetic function reflected this remarkable structural preservation.

**Lipidomic comparison of *Chroococcidiopsis* and *Synechocystis* upon desiccation conditions and in response to temperature variations.**

We determined the first complete lipidome of *Chroococcidiopsis* after lipid extraction, separation by 2D TLC and analysis of all major lipid classes by GC-MS after mass fragmentation analyzed with an ion trap. We could detect the four most abundant and conserved lipids of cyanobacteria, *i.e.* the two galactolipids, MGDG and DGDG, the sulfolipid SQDG, and the phospholipid PG (Supplemental Table S1; Fig. 5). We did not detect MGlcDG, which is an immediate precursor for the production of MGDG and is usually a minor component of cyanobacteria lipidome. Lipid class molecular species of *Synechocystis* were consistent with previous characterizations (Hewelt-Belka et al. 2020; Mavroudakis et al. 2019; Plohnke et al. 2015; Yuzawa et al. 2014). We then used these lipid class molecular species to perform quantitative profiling by LC-MSMS, as described previously (Pittera et al. 2018) and compared both cyanobacteria strains upon dehydration on gypsum surface, at 25°C, in above detailed conditions (Fig. 5A). Total lipid extraction yield from gypsum surface being unknown, we did not analyze the evolution of whole lipidome quantities. The first point corresponded to 2 days of incubation at the surface of gypsum to take into account an identical treatment of all samples. In addition to resistance to desiccation, we analyzed the response of *Chroococcidiopsis* to temperature variations. To that purpose, we cultivated cells in liquid BG11 medium at 15°C, 25°C and 35°C. We controlled the photosynthetic efficiency of these cultures at various temperatures and noted that *Chroococcidiopsis* Fv/Fm was always higher as that measured in *Synechocystis*, and remarkably more stable (Fig. 3B). We then analyzed the lipidome profile after two days of acclimation at each temperature (Fig. 5B). In all conditions, *Chroococcidiopsis* contained proportionally more MGDG than *Synechocystis* analyzed in parallel (Fig. 5).

Figure 5

In both species, dehydration led to a rapid decrease of MGDG and DGDG proportions (Fig. 5A). It must be noticed that *Chroococcidiopsis* kept a higher basal level of MGDG, around 7-12 mol%, compared to *Synechocystis*, with <2.5 mol% MGDG after three weeks of dehydration (Fig. 5A). In both species, SQDG proportion increased in the course of desiccation, becoming the most abundant lipid class, reaching its maximum value in *Synechoscystis* within the first week, whereas its

adjustment was more progressive in *Chroococcidiopsis*. To our knowledge, this striking remodeling of cyanobacteria membrane lipids appeared as specific to desiccation.

By contrast, when acclimated to temperatures ranging from 15 to 35°C in liquid conditions, less membrane lipid variations could be observed (Fig. 5B). Such moderate change in lipidome profile with temperature was reported in the comprehensive analysis of marine *Synechococcus* ecotypes populating oceans at various latitudes. In *Synechococcus*, thermoacclimation and adaptation was rather visible by qualitative changes within each lipid class, by a remodeling of fatty acid chain-length and desaturation levels (Pittera et al. 2018). We sought if similar responses could be detected here.

Upon desiccation, *Synechocystis* highlighted intense changes in acyl chain-length and desaturation levels in all its lipid classes. In MGDG (Fig. 6A), the major diacyl molecular species, namely MGDG-34-3 (with a sum of carbon of 34 and 3 double bonds), making more than 40% of this lipid class at D0, dropped to ~10% after three weeks of desiccation. A similar decline of MGDG-34-4 was observed. Meanwhile, MGDG-32-0 molecular species increased, as well as other more saturated molecular species. By contrast, *Chroococcidiopsis* MGDG was strikingly stable, besides a slight decrease of MGDG-34-4. Likewise, DGDG, SQDG and PG acyl profile were strongly altered in *Synechocystis* in the course of desiccation, whereas little change could be noticed in *Chroococcidiopsis* (Fig. 6A, C and D). This suggests that *Chroococcidipsis* does not adjust its lipid properties *via* the regulation of desaturases.

Figure 6

We verified if such unique feature could also be observed in response to temperature variations. We analyzed the molecular species of MGDG, DGDG, SQDG and PG in both cyanobacteria species after a cultivation at 15°C, 25°C and 35°C (Fig. 7). In *Synechocystis,* MGDG is marked by a decline of MGDG-34-3 and MGDG-34-4 with increasing temperature, and an increase in more saturated species such as MGDG-30-0 (Fig. 7A). Similarly, DGDG-34-2, DGDG-34-3 and DGDG-34-4 decrease whereas more saturated species increase (Fig. 7B); SQDG-34-3 decreases whereas SQDG-34-1 increases (Fig. 7C); and PG-34-3 decreases whereas more saturated species increase (Fig. 7D). This tuning of glycerolipid molecular species based on a balance between saturated and unsaturated lipids fits with a mechanism described previously in *Synechocystis* PCC 6803, also known as a homeoviscous acclimation mechanism, where membrane fluidity is maintained at lower temperature by increasing the number of double bonds on acyl chains (Laczko-Dobos and Szalontai 2009). By contrast, *Chroococcidiopsis* exhibits a striking compositional stability of MGDG, DGDG and SQDG (Fig. 7A, B and C). Only PG shows a decline of PG-31-0, PG-36-2 and PG-36-3 and an increase of PG-37-2 and PG-38-2 at higher temperature, possibly responding to temperature variations at the level of acyl chain length, rather than by controlling desaturation level (Fig. 7D).

Figure 8

Altogether, these results show that *Chroococcidiopsis* respond specifically to desiccation by adjusting the relative proportion of its membrane lipids, with SQDG becoming the most prominent lipid class, and keeping a basal level of galactolipids (Fig. 6). Surprisingly, *Chroococcidiopsis* lacks the homeoviscuous acclimation mechanism known in most prokaryotic and eukaryotic organisms studied to date, in which membrane fluidity is maintained by tuning the relative proportions of saturated and unsaturated lipids in response to temperature variation (Fig. 7).

Intriguingly, the conservation of the membrane lipid composition of *Chroococcidiopsis* exposed to variable temperatures correlated with a stable Fv/Fm measurement (Fig. 3B), whereas compositional changes upon desiccation, preserving a basal level of MGDG and DGDG, correlated with a decline of

Fv/Fm, still preserving a basal level of photosynthesis efficiency (Fig. 3A). We refined therefore our analysis of photosynthetic function.

**PSI and PSII fluorescence emission spectra at -77K of *Chroococcidiopsis* and *Synechocystis* upon desiccation conditions and in response to temperature variations.**

We refined our analysis of photosynthetic machinery functional integrity by analyzing chlorophyll fluorescence emission spectroscopy at 77 K. At low temperature, biochemical and physiological processes that modulate fluorescence are abolished, and the fluorescence emission of both photosystem I (PSI) and (PSII) become distinguishable (Brody 1958; Lamb et al. 2018; Murata et al. 1966).

The fluorescence curves show that *Synechocystis* PCC 6803 has two close signals at 650 nm and 662 nm (Fig. 8A and C) that correspond to the peaks of free phycobilisome allophycocyanin (APhyC) (Shen and Vermaas 1994). *Chroococcidiopsis* G-MTQ-3P2 also exhibits two peaks, slightly shifted at 646 nm and 669 nm (Fig. 8B and D), highlighting differences in antenna complex proteins. A peak at 655 nm in *Synechocystis* can be attributed to free phycocyanin (PhyC) (Ossenbuhl et al. 2006; van Stokkum et al. 2018); *Chroococcidiopsis* does not show any such peak suggesting the existence of a more efficient electron flow powered within phycobilisomes. PSII peaks at 686 nm and 693 nm characterized in *Synechocystis* can be observed almost at the same position in *Chroococcidiopsis*, *i.e.* at 687 nm and 694 nm respectively. Peaks linked to PSI are observed at 721 nm and 724 nm in *Synechocystis* and *Chroococcidiopsis* respectively. The excitation being set at 570 nm, all the observed signals reflect mainly the energy transmission from phycobilisomes to photosystems.

Figure 8

The acclimation of *Synechocystis* cultures at increasing temperatures (Fig. 8A) led to a slight increase of the PSI/PSII peak ratio. In comparison the PSI/PSII fluorescence emission ratio in *Chroococcidiopsis* remained >1 in every condition (Fig. 8B), supporting the existence of a stronger photosynthetic alternative electron flow powered by the phycobilisomes as compared to *Synechocystis*, and a decrease of the PSII activity, either by photodamage or specialization. Such behavior has been reported in a thermophilic *Synechococcus* in high light (Kilian et al. 2007) with a strong rearrangement of the complexes. Interestingly the Fv/Fm results we measured (Fig. 3B) was unaffected by temperature variations, and thus contradicts the existence of any significant photodamage. Altogether, presented results suggest therefore a strong PSII/phycobilisome rearrangement in *Chroococcidiopsis* when temperature increases. The (APhyC/PhyC)/PSII fluorescence emission ratio was comparable in both strains grown at 25°C. While in *Synechocystis* this ratio seemed stable with increased temperature, in *Chroococcidiopsis* it strongly decreased, suggesting a loss of free phycobilisomes or possibly their conjugation with the photosystems. Taken together with the stable Fv/Fm values at increasing temperatures, these results suggest a disassembly / re-assembly of the phycobillisome complexes. Such supramolecular rearrangement may allow *Chroococcidiopsis* to cope with fluctuating metabolic speed, preventing or limiting damages to the photosystems linked to the accumulation of reducing equivalents.

During dehydration at the surface of gypsum, *Synechocystis* fluorescence curves exhibited a modification of the free phycobilisomes peak after two weeks, where the 2 lateral peaks of presumably free APhyCs decrease (Fig. 8C). At this stage a Fv/Fm signal was weak but could still be detected (Fig. 3A). The Fv/Fm signal was abolished after three weeks of dehydration (Fig. 3A) and the low temperature fluorescence profile demonstrated a complete collapse (Fig. 8C), with a de-connection of the phycobilisomes from the photosystems, accompanied by a shift of the free phycobilisome peak toward longer wavelengths. By contrast, *Chroococcidiopsis* seemed to respond

9

to desiccation by slowly detaching its phycobilisomes from both PSI and PSII (Fig. 8D), which could be considered either as a preparation or as an organized reaction to the stress. It is important to point out that all along the dehydration process, *Chroococcidiopsis* could rapidly recover some low level of photosynthetic activity (Fig. 3A).

**Photosynthetic pigment profiles in *Chroococcidiopsis* and *Synechocystis* in response to temperature variations.**

Since intense rearrangements of photosystems occurred during desiccation, leading likely to a complete collapse of the photosynthetic machinery in *Synechocystis*, and possibly in the direction of a long-term resistance to high temperature in *Chroococcidiopsis*, we analyzed photosynthetic pigment profiles (Supplemental Fig. S2). We did not analyze cell wall specific pigments such as scytonemin involved in UV protection (Casero et al. 2021). We did not detect chlorophyll *f*, reported earlier in *Chroococcidiopsis thermalis* (Nurnberg et al. 2018). Peaks were assessed by comparison with standards and the profile was analyzed based on relative values integrating peaks measured at $A_{450}$. Relative changes can therefore be deduced, but their magnitude cannot be quantified.

In *Synechocystis*, the temperature treatments did not reveal any important change in the pigment composition (Supplemental Fig. S2A). By contrast, *Chroococcidiopsis* adapted its chlorophyllide *a*, and increased its conversion to chlorophyll *a* with increasing temperature (Supplemental Fig. S2B). This behavior could be linked to the increased demand for reducing power by ramping up metabolic speed with higher temperature.

Lutein and echinenone both decreased in *Chroococcidiopsis* grown at higher temperature, while canthaxanthin was significantly increased. Lutein was observed to be linked to energy dissipation in plants (Jahns and Holzwarth 2012), accepting electrons from excited chlorophyll in antenna complexes and dissipating its energy. The orange carotenoid protein (OCP) binds echinenone and hydroxy-echinenone as well as canthaxanthin; it is known to bind phycobillisonmes and quench their excitation energy usually transferred to the photosystems when reduced (Kirilovsky and Wilson 2007). The replacement of the single OCP pigment from echinenone to canthaxanthin promotes a faster reduction of the protein but delays the phycobilisome quenching activity *in vivo* (Leverenz et al. 2015) independently of the redox status of the electron transfer chain. Such modification is observed in our pigment profile changes, suggesting an active regulation mechanism, limiting energy dissipation, in *Chroococcidiopsis* while absent in *Synechocystis*.

**Photosynthetic pigment profiles in *Chroococcidiopsis* and *Synechocystis* upon desiccation conditions.**

The three-week slow desiccation of cyanobacteria at the surface of gypsum led to intense phenotypic differences described above. The profile shown in Supplemental Fig. S2A corresponds to *Synechocystis* sub-lethal condition. When dehydrated, *Synechocystis* accumulated an uncharacterized myxol derivative *a*, which initial level, below detection, increased to such an extent that it became the major pigment. Coincidentally, a deoxy-myxol derivative *b*, canthaxanthin and 3-hydroxy-echinenone also increased while cells lost chlorophyll *a*, zeaxanthin and another deoxy-myxol derivative *c*. In *Chroococcidiopsis*, deoxy-myxol derivative *a*, decayed under the detection level while the deoxy-myxol derivative *b*, which was in low abundance, became a strongly dominant pigment (Supplemental Fig. S2A), a similar trend as that observed in *Synechocystis* for the later but is completely opposite for the former. The myxol derivative pigments were previously reported to be linked to stress adaptation in cyanobacteria (Kosourov et al. 2016). Synechoxanthin and myxoxanthophyll were shown to be mildly involved in high light resistance in *Synechococcus* (Zhu et al. 2010). Myxol-derivative 1 related to myxoxanthophylls accumulated abundantly in

*Chroococcidiopsis* after three weeks of desiccation and remained minor in *Synechocystis*; this pigment may be involved in the cell wall organization and help absorbing harmful radiation when the cell metabolism is low (Mohamed et al. 2005), possibly acting in synergy with scytonemin (Casero et al. 2021). Additionnally, myxoxantophylls are also involved in the assembly of some antenna like proteins (Proctor et al. 2020). Such rearrangement of myxoxantophylls confirms the intensity of the stress experienced and again suggests a completely different response of the two strains tested here.

In *Synechococcus*, the combined depletion of zeaxanthin, cryptoxanthin, echinenone and hydroxy-echinenone renders the cells very sensitive to high light (Zhu et al. 2010). Chlorophyll-derived pigments decreased in *Synechocystis*, consistently with the degradation of photosynthetic light harvest. Deoxy-myxol derivatives, canthaxanthin and 3-hydroxy-echinenone are the last remnants of the photosynthetic machinery and their presence as the major pigments after dehydration demonstrate the focus of the cell strategy on dissipating most of the received energy likely in response to an arrested metabolism. It could be postulated that the small amount of light harvest by chlorophyll triggered oxidation events during dehydration or during the first instants of re-hydration, stages where the quenching and repair mechanisms are not functional. *Chroococcidiopsis* exhibits a similar strategy but the chlorophyll decrease led to their complete disappearance. Similarly some (deoxy)myxol derivatives accumulated during dehydration, the quenching mechanism by lutein appeared to be replacing echinenone and canthaxanthin, targeting excited chlorophylls as described above. Considering the survival of *Chroococcidiopsis* and the death of *Synechocystis* after three weeks of desiccation, it could be speculated that the resistance to dehydration might include the capacity to actively sense the stress and suppress chlorophylls before the drought-linked metabolic arrest, highlighting a likely role of certain myxol derivatives in quenching the excessive excitation energy in these conditions.

**Discussion.**

**Endolithic *Chroococcidiopsis* G-MTQ-3P2 is not capable of extracting water from gypsum rocks, even upon long dehydration periods.**

We tried to repeat past experiments showing that, upon desiccation, *Chroococcidiopsis* G-MTQ-3P2 isolated from gypsum rock in the Atacama desert could extract water from gypsum crystals, leading to the formation of anhydrite (Huang et al. 2020). No sign of water extraction could be observed under exposure to cyanobacteria of polycrystalline gypsum chips of (010) or (011) faces of single crystals (Fig. 1 and Supplemental Fig. S1). Our results are in line with previous skeptical comments on this supposed property, both in practical and theoretical terms (Wierzchos et al., 2020). We suppose that in the original work, used gypsum chips were small sized (5 mm x 8 mm) and thin enough (0.5 mm) to allow unspecific losses of water, unrelated to the presence of *Chroococcidiopsis*. Alternatively, the more heterogeneous composition of the natural samples used in previous studies, the presence of multiple species or a particular surface texture could have led to a different result. Nevertheless, based on our in-depth study, *Chroococcidiopsis* is not able to extract water from a gypsum crystal.

**_Chroococcidiopsis_ forms desiccation-resisting cells, preserving thylakoid membrane integrity and a basal level of photosynthesis**

When using *Synechocystis* PCC 6803 as a control desiccation-sensitive strain, analyzed in parallel, major features appeared as specific to *Chroococcidiopsis* G-MTQ-3P2. As expected, *Chroococcidiopsis* cells could resist better to desiccation, recovering and growing even after three weeks of treatment (Fig. 2). The cell wall nature seems heavily modified in *Chroococcidiopsis* (Fig. 4), likely producing extracellular polysaccharides known to be essential in several species to survive long periods of dehydration (Tamaru et al. 2005) and proposed to have ROS scavenging activities (Wang et al. 2022). The recovery was not immediate, with a lag of about four days, suggesting the formation a desiccation-resisting stage that needed to be converted back into a vegetative form as reported for other cyanobacteria (Sauer et al. 2001; Spat et al. 2018). The pigmentation of cyanobacteria at the surface of gypsum (Fig. 1) suggested a bleaching of chlorophyll and a disintegration of photosynthetic antenna in *Synechocystis*, whereas *Chroococcidiopsis* pigmentation was modified toward a brownish color, likely a more heat-dissipating tint. Consistently, the photosynthetic efficiency measured by the Fv/Fm ratio suggest a complete collapse of PSII in *Synechocystis*, whereas that of *Chroococcidiopsis* dropped, but remained to a low basal level (Fig. 3). STEM analyses suggest that the *Chroococcidiopsis* desiccation-resisting stage accumulates some form of intracellular reserves (Fig. 4), which needs to be characterized in the future, and exhibits a striking preservation of thylakoid membrane integrity. By comparison, *Synechocystis* cells also show some kind of cytosolic granule formation, but the thylakoids appear as disorganized.

**The anionic sulfolipid SQDG plays a critical role in the response of cyanobacteria to desiccation, likely involved in membrane structure preservation**

We sought some possible changes of membrane lipid profiles that could suggest some specific lipidomic response triggered in *Chroococcidiopsis*, allowing the preservation of thylakoid architecture. After determining the complete lipidome of the studied strains (Supplemental Table S1), we first analyzed the relative proportion of lipid classes in total extracts from both species. Although this analysis is based on whole cell extracts, lipid profiles mainly reflect the composition of the major membrane system, i.e. thylakoids. Desiccation had a very strong impact on the relative proportions of MGDG, DGDG, SQDG and PG in both cyanobacteria, marked by a dramatic decrease of

galactolipids, suggesting the activation of a specific catabolic machinery, and an increase of SQDG becoming the most abundant lipid class, just after one week (Fig. 5A).

The biological function of SQDG, a non-phosphorus anionic lipid, in photosynthetic organisms has been very difficult to assess due to the survival of SQDG-synthesizing mutants analyzed to date. It has been proposed that this lipid could be to some extent dispensable (Sato et al. 2016). Cyanobacteria mutants lacking SQDG were either strongly impaired, such as in *Synechocystis*, or had no apparent phenotype under optimal growth condition, such as in *Synechococcus* (Aoki et al. 2004; Apdila and Awai 2018; Guler et al. 1996). Some marine cyanobacteria were shown to contain high levels of SQDG (Van Mooy et al. 2006), suggesting a correlation of SQDG with high salinity, and may be related to the role of this lipid in desiccation highlighted here. One environmental context highlights a role for SQDG, upon phosphate shortage, when PG, another anionic lipid containing a phosphate group, decrease and is replaced by the sulfolipid (Bolik et al. 2022; Boudiere et al. 2014; Frentzen 2004; Shimojima 2011).

Early cyanobacteria lacking thylakoid membranes, such as *Gloeobacter*, had no SQDG (Sato and Awai 2016; Sato et al. 2016). The acquisition of SQDG in cyanobacteria coincides with the emergence of thylakoid membranes, and it was recently proposed that this gain had been critical in the sustained production of an anionic bilayer-forming lipid, even in a low-phosphate environment, allowing thylakoid membranes to be produced (Gueguen and Marechal 2021). This role of SQDG as a key bilayer-forming lipid for the maintenance of thylakoids under stress appears even more vividly here, upon desiccation conditions (Fig. 5A). Very little studies report on potential lipidome remodeling upon drought or desiccation. Based on metabolic labelling analysis, the desiccation-tolerant cyanobacterium *Nostoc commune* was shown to synthesize SQDG and PG within minutes after rehydration, where 2 hours were necessary to recover a production of MGDG and DGDG, consistently with the preservation of an active SQDG synthesis system in the desiccation-resisting cells (Taranto et al. 1993). It was also reported that water deficit induced an accumulation of SQDG in drought-resistant plants, and a drastic decrease in sensitive ones (Okanenko et al. 2003; Taran et al. 2000). In both *Synechocystis* and *Chroococcidiopsis*, SQDG increased strikingly upon desiccation (Fig. 5A), so this increase may not be sufficient to allow cells to cope with long periods of dehydration. It is possible that the preservation of a minimal production of MGDG in *Chroococcidiopsis* allows maintaining a sufficient level of this galactolipid to generate photosynthetic membranes. Indeed, this lipid does not spontaneously form membrane bilayers, but a structure known as Hexagonal II phase (Jouhet 2013). Such Hexagonal II phase forming lipid was recently proposed to play a central role in initiating the formation of thylakoids in cyanobacteria, via a non-vesicular mechanism, as long as such lipid as SQDG was present (Gueguen and Marechal 2021). The lipid profile of desiccated *Chroococcidiopsis* cell (Fig. 5A) is consistent with this model.

**_Chroococcidiopsis_ membrane lipids do not exhibit any homeoviscuous adaptation mechanism in response to temperature variations or desiccation.**

When analyzing *Synechocystis* and *Chroococcidiopsis* at increasing temperature, further phenotypic differences were observed. We initially hypothesized that *Chroococcidiopsis* would exhibit an elaborate tuning of its fatty acid composition in lipid classes, with a homeoviscuous acclimation mechanism (Laczko-Dobos and Szalontai 2009; Pittera et al. 2018), allowing an adjustment to temperature variations occurring in desert lands. Previous analysis on the effect of temperature variations on the cyanobacteria *Synechococcus* showed that little change was observed on the relative proportions of each lipid class, whereas major changes occurred within each class at the fatty acid composition level (Pittera et al. 2018). Both *Synechocystis* and *Chroococcidiopsis* also showed little changes in their lipid class profiles in response to temperature variation (Fig. 5B). However,

whereas *Synechocystis* exhibited a classical homeoviscuous acclimation at the level of its fatty acids in its membrane lipids, *Chroococcidiopsis* did not show any strong change from 15°C to 35°C (Fig. 7B). Actually, *Chroococcidiopsis* acyl profiles in each lipid classes (Fig. 7) did not show any spectacular variations in all tested conditions.

Homeoviscuous acclimation is supposed to maintain a level of lateral fluidity preserving essential biological function including photosynthesis. Surprisingly, the existence of this specific lipid remodeling mechanism in *Synechocystis* does not prevent changes in Fv/Fm, impaired by cultivation at lower temperature (Fig. 3B). By contrast, *Chroococcidiopsis* laking this classical response preserve a high PSII efficiency at all tested temperatures (Fig. 3B). Therefore *Chroococcidiopsis* adaptation to desert conditions, i.e. low humidity level, highly variable temperatures and high light irradiance, does not involve a classical mechanism enhanced to perform better in these conditions, but rather a unique series of adaptive systems, likely to have diverged from the cyanobacteria core ones.

### *Chroococcidiopsis* remodels its photosynthetic machinery upon environmental changes.

When we compared the effect of acclimation to different temperatures on photosynthesis function, we observed a strong stability of *Chroococcidiopsis* photochemistry at all temperatures (Fig. 3B) linked with a very dynamic pigment adjustment (Supplemental Fig. S2). *Chroococcidiopsis* seems to remodel the light harvesting components of its photosynthetic machinery to maintain a maximal level of energy capture, likely by the tuning of chlorophyllide conversion into chlorophyll (Supplemental Fig. S2). In wheat, the conversion of protochlorophyllide to chlorophyll by the chlorophyll synthase was shown to be blocked at low temperatures (Liu et al. 2012), suggesting a similar mechanism in other photosynthetic organisms. By contrast, *Synechocystis* seems unable to a similar pigment adjustment, and this likely affects negatively its photosynthetic efficiency when temperature decreases (Fig. 3B). Analyses of *Synechococcus* (Li et al. 2019) and *Anabaena* (Klodawska et al. 2019) over a wider temperature range suggest that the amount of chlorophyll in cyanobacteria is maximal around the optimal growth temperature. We may postulate that *Synechocystis* also contains a chlorophyll level adapted to its temperature preferendum, whereas *Chroococcidiopsis* is capable of tuning it to cope with a wider range of temperature, encountered daily and seasonally in desert lands.

The low temperature spectrum analysis made after acclimation is consistent with a stability of the phycobilisome energy transfer in *Synechocystis* (Fig. 8A), whereas an adjustment of the excitation energy distribution is observed in *Chroococcidiopsis* (Fig. 8B). *Chroococcidiopsis* pattern reflects strong variations at the level of the free antenna but seem independent from energy quenching mechanism based on the PSI cyclic electron flow, vastly documented in higher plants and microalgae (Campbell and Oquist 1996). It suggests also an absence of effect on the redox state of the plastoquinone (PQ) pool that would quench PSII excitation (Mullineaux et al. 2018). It must be pointed out that even if PSI binds to 85% of the total chlorophyll A molecules in cyanobacteria (Renger 2007), the *Chroococcidiopsis* low temperature spectrum does not show any difference in excitation routes linked to an increase in chlorophyll A (Fig. 8B) suggesting a stable PSI/PSII excitation distribution in the endolithic cyanobacterium. A decrease of free phycobilisome peaks (Fig. 8) suggests their coupling with both photosystems in a mechanism reverse to that involved in high light decoupling (Tamary et al. 2012). This behavior could be explained by the increased energy demand by a faster metabolism at higher temperature, therefore otherwise oxidizing the plastoquinone pool.

We compared whole protein profiles of *Synechocystis* PCC 6803 and *Chroococcidiopsis* G-MTQ-3P2 by SDS-PAGE (Supplemental Fig. S3) and identified some of the major polypeptides of *Synechocystis* based on previous characterization (Bolte et al. 2008). The profiles obtained from the two

cyanobacteria grown in control conditions were very different (Supplemental Fig. S3, lanes D0) and it was not possible to assess any of the *Chroococcidiopsis* band unambiguously. Nevertheless, we observed a difference at the level of *Synechocystis* ApcE, an essential anchor protein of the phycobilisomes to the photosynthetic membrane, having ~900 amino acids (Capuano et al. 1991; Elanskaya et al. 2018). Although the sequencing and annotation of *Chroococcidiopsis* G-MTQ-3P2 is still not resolved (Murray et al. 2021), the presence of ApcE in related *Chroococcidiopsis* strains is confirmed based on a similarity search using the *Synechocystis* PCC 6803 sequence (Uniprot ID Q02907) as a query. The predicted size of ApcE being ~130 kDa, its relative abundance seems drastically lower in *Chroococcidiopsis*, compared to *Synechocystis* (Supplemental Fig. S3, lanes D0). This and other apparent differences in relative abundance of major phycobilisome components highlight a huge infrastructural divergence of the photosystems between the two species, which is possibly related to the different behaviors observed on the phycobilisomes assembly-disassembly.

As a general response to stress, cyanobacteria can shift their photosynthetic machinery to a new state, with lower photochemistry, previously described as 'active chlorosis' (Sauer et al. 2001). During dehydration we could observe in the pigment composition analysis that *Synechocystis* maintained a basal level of chlorophyllic pigments while *Chroococcidiopsis* lost most of it (Supplemental Fig. S2). This observation parallels with the very low overall signal obtained in low temperature fluorescence that we unfortunately could not quantify reliably (Fig. 8). As *Chroococcidiopsis* survived desiccation (Fig. 2) and Synechocystis did not, a correlation appears with chlorophyll removal. We thus postulate that the remaining chlorophyll may be responsible for an oxidative stress killing *Synechocystis* cells either during dehydration or at rehydration. It would be interesting to pursue that hypothesis by attempting revival assays in very low light or/and with an external carbon source.

We also observed that desiccation triggered a strong decrease of phycobiliproteins in both *Synechocystis* and *Chroococcidiopsis*. The initial level of phycobiliproteins appear to represent a higher fraction of total soluble proteins in *Synechocystis* compared to *Chroococcidiopsis* (Supplemental Fig. S3, lanes D0), maybe linked to its faster growth rate. During dehydration, the phycobiliproteins of *Synechocystis* almost completely disappeared while *Chroococcidiopsis* retained an apparent basal level (Supplemental Fig. S3, lanes D2 and D15). If we parallel these observations to the strong decrease in chlorophyll content and the low temperature signal, we postulate that these phycobilisomes either re-emit this energy directly as heat or through another acceptor that does so. The overall pigment analysis reveals an enrichment for myxol-derived pigments (Supplemental Fig. S2) possibly responsible for such dissipation, as described above. The color of the dehydrated *Chroococcidiopsis* (Fig. 1) is consistent with that observation. Future studies should address the structure of pigment-binding components and their dynamics in response to environmental stress in *Chroococcidiopsis*.

All results taken together, in acclimation to different temperature and different water availability, *Chroococcidiopsis* differs from *Synechocystis* by the extensive regulation of its phycobilisome energetic conjugation to the photosystems. PSI receives most of this excitation (Fig. 8) suggesting a central role of this photosystem in cellular energetics. It could be postulated that natively, *Chroococcidiopsis* needs a higher ATP/NAD(P)H ratio compared to *Synechocystis*, linked to a higher energy dissipation through "chloro"-respiration (Ogawa et al. 2013). In cyanobacteria, PSI is regulated by its oligomerization, a phenomenon lost in photosynthetic eukaryotes (Li et al. 2014). This regulation is involved in the energy dissipation and involves PsaL, a subunit of PSI binding PsaA and PsaB dimers (Chitnis and Chitnis 1993). This oligomerization was shown to be dependent on the C-terminal part of the PsaL protein (Jordan et al. 2001). In *Synechocystis* PsaL, an aspartic acid

residue is involved in the calcium-dependent trimerization of PSI. *Cyanobacterium aponinum*, a drought resistant cyanobacteria, has a lysine residue at that position, which prevents the binding and is linked to high light resistance (Dobson et al. 2021). The Aspartic acid residue is conserved in *Chroococcidiopsis* PsaL sequences, suggesting an evolution mechanism to survive high light and drought different than that present in *C. aponinum*. Interestingly the PsaB subunit from *Chroococcidiopsis* species also shows a 7-amino-acid insertion compared to *Synechocystis.* This insertion is also present at a similar location in *C. aponinum*. These extra amino acids are located on the stromal side of the protein complex and oriented toward a chlorophyll rich complex region suggesting a role in further complex arrangement. This insertion is located next to the PsaA-PsaB dimer interface (Semchonok et al. 2022) and may be involved in the interaction of PsaA with other proteins like IsiA, having a role in energy dissipation (Kouril et al. 2005; Toporik et al. 2019) or oxidative stress management (Michel and Pistorius 2004). Future works are needed to evaluate this hypothetical molecular determinant of *Chroococcidiopsis* remarkable adaptation of its photosynthetic machinery to desiccation conditions.

**Conclusions.**

This work explores some biological traits of the endolithic cyanobacterium *Chroococcidiopsis* G-MTQ-3P2 discovered under the surface of gypsum rocks in the Atacama desert, in laboratory conditions where desiccation was performed on the same mineral surface. We refuted previous studies supporting that development at the surface of gypsum would allow this cyanobacteria to extract water from the gypsum surface, so we do not provide any clue on the specificity of the development of this strain on such mineral. Our work suggests a critical and overlooked role of the sulfolipid SQDG upon desiccation in cyanobacteria, but since gypsum is sulfur rich, this response should also be evaluated in desiccation experiments performed on sulfur-poor minerals. The adaptation of *Chroococcidiopsis* to desiccation and temperature variations in arid areas did not correspond to a 'more efficient' or 'enhanced' mechanism present in cyanobacteria populating temperate regions such as the freshwater *Synechocystis* PCC 6803 strain. In particular, *Chroococcidiopsis* remodels only moderately its acyl-profile in lipid classes, lacking therefore the classical homeoviscuous thermoacclimation system. Rather, it maintains its lipid molecular species in most circumstances. This could be considered a weakness, but the photosynthetic machinery proved to be particularly resilient, owing to distinct structural and functional organization compared to *Synechocystis*. Indeed, *Chroococcidiopsis* proved to be extremely performant in maintaining on optimal level of light energy capture and conversion. Regarding photosynthesis machinery functioning and acclimation to desiccation, future investigations are necessary to dissect the mechanisms responsible for the differences we observed. One may wonder why endolithic *Chroococcidiopsis* strains, if so performant and resistant to desiccation, are not encountered more often in most known habitats. The *Chroococcidiopsis* phylum is spread in hot and cold deserts wordwide (Bahl et al. 2011; Lacap-Bugler et al. 2017), but its presence declines when water availability increases (Hagemann et al. 2015). A hypothesis not evaluated here may be that these *Chroococcidiopsis* have an Achilles' heel, i.e. their sensitivity to high light irradiance. A rich literature addresses their resistance to UV radiation, and focuses on the hypothetical capacity of such microorganisms to survive on other planets, such as Mars (Billi et al. 2022; Billi et al. 2019; Cockell et al. 2005; Fardelli et al. 2023; Friedmann and Ocampo-Friedmann 1995; Gomez-Silva 2018; Li et al. 2022; Rzymski et al. 2022; Verseux et al. 2017). It seems that a lot needs to be done to understand this unique lifestyle on planet Earth. The recent description of a *Chroococcidiopsis* strain isolated from a solar panel (Baldanta et al. 2023), resisting also to high UV-C, may help comprehend the different strategies in the *Chroococcidiopsis* to cope with high light intensities. In the context of climate change, this work thus suggests that temperate cyanobacteria may be unable to evolve in the direction of a high tolerance to arid land conditions,

using the adaptation and acclimation mechanisms occurring in extant endolithic cyanobacteria. A low moisture threshold may provoke the extinction of species, and their replacement by novel microbial communities. To have a more complete overview, this work should nevertheless be completed with a study of desiccation-tolerant cyanobacteria also living in temperate regions such as *Nostoc*. The efficiency of colonization of emerging arid areas by pioneering *Chroococcidiopsis* needs also to be addressed.

## Material and methods

**Strains and culture conditions.** *Chroococcidiopsis* G-MTQ-3P2 was obtained from J. DiRuggiero and maintained in BG11 growth media according to previous works (Huang et al. 2020). The strain identification was verified by sequencing the 16S rRNA that matched the published genome (Huang et al. 2020; Murray et al. 2021) and grouped with other *Chroococcidiopsis* species on a neighbor joining tree. The study of *Chroococcidiopsis* G-MTQ-3P2 was performed in parallel with a dehydration sensitive cyanobacteria, *Synechocystis* PCC 6803 (Raanan et al. 2016). To sustain the autotrophic metabolism of the cyanobacterial strains and maintain a stable pH at 7.5, culture was performed with a 2 mM inorganic carbon supply, under 3,000 ppm $CO_2$ bubbling. A photosynthetic fluorescence kinetics with an Fv/Fm ratio of 0.47 +/-0.02, determined as described below, was considered as an initial physiological condition for experiments. Cell density assessment was required to monitor cultures performed in biological replicates. Due to *Chroococcidiopsis* tendency to form aggregates, the spectrophotometric measure of total chlorophyll was performed with a 24-h methanol extraction and quantified as described previously (Lichtenthaler and Wellburn 1983).

**Inoculation and incubation of gypsum chips flat surfaces.** Dehydration assays were performed on pure gypsum (rehydrated plaster, alpha plaster made from Molda Super provided by SAINT GOBAIN PLACO). Gypsum polycrystalline chips consisted of 15 mm diameter discs, with 2 mm thickness, UV-sterilized. Liquid cyanobacterial cultures were concentrated to reach 200 µg Chlorophyll.mL$^{-1}$ in BG11, from which 100 µL were deposited on the surface of a chip in a sterile 6-well (20 mm diameter) cell culture plate (Greiner) and immediately covered. The chips being porous, the media quickly diffused in while the cells remained at the surface. Obtained chips were placed under a constant 20 µE (µmol photon.m$^{-2}$.s$^{-1}$) fluorescent tube light at 25°C according to previous studies (Huang et al. 2020). A water layer was added at the bottom of the incubation chamber during the incubation period, preventing a complete desiccation of samples in the initial hours of the treatment, but not preventing the complete desiccation after a few days. Alternatively, a centimetric gypsum rock single crystal from San Martin de la Vega quarry (Spain) was provided by SAINT GOBAIN PLACO, France. The determination of the orientation of the crystalline lattice was performed using an X-Ray Laue diffractometer. With the help of J. Debray (Neel Institute, CNRS, Grenoble) the crystal was cut so as to expose the (011) surface on several 1-cm² pieces. Crystal cut so to expose the (010) surface was used as a control. The obtained chips were treated and inoculated as above.

**XRD analysis of gypsum phase transition into anhydrite.** The crystalline structure of pristine gypsum and anhydrite as well as inoculated gypsum was determined by means of X Ray diffraction (XRD) to assess potential phase transition in gypsum. A Panalytical Empyrean diffractometer equipped with a Cobalt X-Ray source was used in a parallel beam configuration, well adapted to the roughness of the polycrystalline gypsum chips. The samples of scraped powder from (011) and (010) monocrystalline gypsum faces were measured on a Bruker D8 diffractometer in Bragg-Brentano geometry with Copper K$\alpha$ radiation. For the sake of clarity, the diffraction patterns are all presented as a function of the scattering angle for Copper K$\alpha$ radiation.

**Photosynthetic efficiency.** In routine, photosynthesis parameters were measured in cell cultures with room temperature fast chlorophyll fluorescence kinetics using a PSI Fluor pen FP110, after 5 min dark relaxation for all culture samples, as described previously (Strasser et al. 2000). The steady-state fluorescence in dark-adapted cultures is termed *F0*, *Fm* is the maximal fluorescence after a saturating light pulse with green light, and *Fv* is the difference between *Fm* and *F0*. With these parameters, the maximum efficiency of energy conversion by photosystem II (PSII) can be calculated as *Fv/Fm*. In the case of fully dehydrated gypsum discs, samples were re-hydrated with distilled water in the dark for 30 min prior the measure.

**Chlorophyll fluorescence emission spectroscopy at 77 K.** Low Temperature Fluorescence was measured using an ocean optics USB2000+ mini spectrophotometer, assorted with a 572 nm band pass filtered white LED, used as excitation. Cells grown in liquid culture were collected by centrifugation at 10,000 x g, for 5 min, in the dark. The pellet was suspended under 50 µmol photon.m$^{-2}$.s$^{-1}$ white light and deposited in the sample holder with a glass cover slide in exactly 1 minute. The sample holder was then closed and immediately plunged into liquid nitrogen. The solid samples being flat gypsum discs, they were directly placed into the sample holder with their cover slide and plunged into liquid nitrogen. The average of 3 biological replicates was represented in all samples.

**Analysis of pigments.** Pigments were analyzed by high performance liquid chromatography (HPLC) (Varian ProStar 800, Walnut Creek, CA, USA) coupled to a diode array detector using a C30 column (Macherey-Nagel), at a 1 mL.min$^{-1}$ flow rate. Cell pellets or gypsum chips with dry sample were suspended in 100 µL of distilled water on ice for 1 minute, then completed up to 1 mL with methanol, bubbled with argon for 1 min and left at -20°C for a week. The methanol extract was dried under argon and suspended in 150 µL N,N-dimethylformamide (DMF), centrifuged at 10,000 x g for 5 min, and prepared into HPLC vials with insert. 50 µL were injected into a C30 column. The elution was followed spectrographically from 260 nm to 680 nm. The elution buffers (A, 80% MeOH, 0.2% NH$_4$-Acetate; B, MeOH; C, Tert-Methyl-Butyl-Ether) were mixed 5% A + 95% B linearly replaced by 5% A + 80% B + 15% C until 10 min, then linearly replaced by 5% A + 30% B + 35% C until 35 min runtime. Results obtained were compared to pigment determined in cyanobacteria and algae (Komatsu et al. 2016; Mochimaru et al. 2008; Taniguchi and Lindsey 2021; Xiong et al. 2017) and extracts of *Arabidopsis thaliana* and *Solanum licopersicum*, allowing peak attribution. Canthaxanthin was confirmed by electrospray ionization ion-trap mass spectrometry (Amazon SL, Bruker; Lipang Platform, Grenoble). Quantification was performed through peak deconvolution using the Fityk software (https://fityk.nieto.pl, 1.3.1 version) in split-gaussian mode on 3 biological replicates, using the 450 nm elution spectrum. In the absence of absorption coefficient available for most compounds in the solvent mix used, relative quantification was performed considering peak area.

**SDS-PAGE**. Cell pellets or dry materials collected from gypsum chips were suspended in 200 µL lysis buffer (urea 8 M, Tris-HCl 50 mM pH 6.8, ethylene glycol-bis(β-aminoethyl ether)-N,N,N',N'-tetraacetic acid 1 mM, and beta-mercaptoethanol 20 mM) and kept on ice. Using about 200 µL of 425-600 µm acid-washed glass beads, the samples were processed using a Precellys24 cell disruptor, with 3 x 30-second runs separated by 30-second pauses in a cold room. After cell disruption, SDS was added (1% final) and the suspension was mixed vigorously using a vortex, incubated 5 min at 80°C, and centrifuged at 10,000 x g for 5 min. The supernatant was collected and proteins were quantified using the Pierce Detergent Compatible Bradford Assay Kit from Thermo Scientific. 20 µg of total proteins were loaded onto a 4-12% pre-cast MES-SDS PAGE gel (Sigma-Aldrich). After migration, the gel was stained using instant Coomassie blue reagent (Sigma-Aldrich).

**Cyanobacteria survival assessment.** The survival of cyanobacteria at the surface of gypsum was assayed by transferring chips into 50 mL of liquid BG11 medium. After 24 hours, cells and gypsum micro-particles were suspended into the growth medium, and the clean chips were then removed with tweezers. The growth rate was followed by chlorophyll quantification as described above.

**Sample chemical preparation for scanning transmission electron microscopy (STEM).** After 21 days of drying onto a gypsum chip, both samples were rehydrated with a drop of 0.1 M phosphate buffer (PB) (pH 7.4), scraped and fixed in 0.1 M PB (pH 7.4) containing 2.5% glutaraldehyde. Under liquid conditions both samples were centrifuged at 1000 g for 5 min and the pelleted cells were fixed in 0.1 M PB (pH 7.4) containing 2.5% glutaraldehyde. All samples in both liquid condition and following

three weeks of desiccation were then prepared as previously described (Flori et al. 2018). Samples were then washed five times in 0.1 M PB (pH 7.4). Samples were fixed by a 2-h incubation on ice in 0.1 M PB (pH 7.4) containing 2% osmium and 1.5% ferricyanide potassium before being washed five times with 0.1 M PB (pH 7.4). Samples were resuspended in 0.1 M PB (pH 7.4) containing 0.1% tannic acid and incubated for 30 min in the dark at room temperature. Samples were again washed five times with 0.1 M PB (pH 7.4), dehydrated in ascending sequences of ethanol, and infiltrated with ethanol/Epon resin mixture. Finally, the samples were embedded in Epon. Ultrathin sections (70–90 nm) were prepared with a diamond knife on a PowerTome ultramicrotome (RMC products, Tucson, AZ, USA) and collected on 200 mesh copper grids. Samples were visualized by scanning transmission electron microscopy (STEM) using a MERLIN microscope (Zeiss, Oberkochen, Germany) set up at 30 KV and 240 pA.

**Lipid extraction.** *Chroococcidiopsis* and *Synechocystis* cells were harvested by centrifugation if collected from a liquid culture, or by placing inoculated chips in 50 mL falcon tubes, and stored at −80°C until analysis. Membrane lipids were extracted in glass hardware following a modified version of the Bligh and Dyer (Bligh and Dyer 1959) procedure, using methanol/dichloromethane/water at ratios of 1.1/1/1.4, then evaporated under nitrogen and stored at −20°C until analysis.

**Fatty acid regiolocalization on glycerolipid classes of *Chroococcidiopsis*.** We first identified the positional distribution of the acyls groups esterified to the main glycerolipids of *Chroococcidiopsis*. To that purpose, cultures grown as described were harvested and the lipids extracted. The glyceroplipid classes were separated by 2D thin layer chromatography on 20 × 20 cm silica plates (Merck, Darmstadt, Germany), using chloroform/methanol/water and chloroform/acetone/methanol/acetic acid/water at ratios of 65/25/4 and 50/20/10/10/5 v/v respectively (Simionato et al. 2011). Glycerolipid spots were revealed under UV light in the presence of 8-anilino-1-naphthalene sulfonic acid (0.2% in pure methanol) and scraped off the plates. Each separated lipid class was recovered from the silica powder after addition of 1.35 ml chloroform:methanol 1:2 v/v, thorough mixing and addition of 0.45 ml chloroform and 0.8 ml $H_2O$ and collection of the chloroform phase. Lipids were then dried under argon and analysed by mass spectrometry (MS). Purified lipid classes were dissolved in 10 mM ammonium acetate in pure methanol. The glycerolipids were introduced by direct infusion (ESI-MS) into a trap type mass spectrometer (Amazon SL, Bruker; Lipang Platform, Grenoble), and their identity was confirmed by MS/MS analysis (Abida et al. 2015). Under these conditions, the produced ions were mainly present as $H^-$, $H^+$, $NH_4^+$ or $Na^+$ adducts. The position of the fatty acid molecular species esterified to the glycerol backbone of the purified glycerolipids was determined by MS/MS analyses. Depending on the glycerolipid species and the ionic adduct, the substituents at *sn*-1 and *sn*-2 positions were differently cleaved on low energy collision-induced dissociation. This was reflected in MS/MS analyses by the preferential loss of one of the two fatty acids, leading to a dissymmetrical abundance of the collision fragments, and following dissociation patterns of $MS^2$ fragments described in previous studies (Abida et al. 2015).

**Lipid quantification.** Cyanobacteria lipid extracts corresponding to about 25 nmol of total fatty acids or to the total extract from the gypsum deposit were dissolved in 100 µl chloroform/methanol [2/1, (v/v)] containing 125 pmol of each internal standard obtained from Avanti Polar Lipids Inc, completed with synthetic standards described previously (Pittera et al. 2018). Lipids were then separated by HPLC using an Agilent 1200 HPLC system with a 150 mm × 3 mm × 5 µm diol column (Macherey-Nagel), at 40°C, and quantified by MS/MS on an Agilent 6460 triple quadrupole mass spectrometer equipped with a jet stream electrospray ion source, as described ealier (Pittera et al. 2018). SQDG analysis was carried out in negative ion mode by scanning for precursors of m/z −225 at a CE of −56 eV. PG, MGDG and DGDG measurements were performed in positive ion mode by scanning for

neutral losses of 189, 179 and 341 Da at CEs of 16, 8 and 8 eV respectively. Quantification was done by multiple reaction monitoring (MRM) of all the molecules detected in the TLC-MS experiment with 100 ms dwell time. Mass spectra were processed with the Agilent MassHunter Workstation software for lipid identification and quantification. Lipid amounts were corrected for response differences between internal standards and external endogenous lipids (Jouhet et al. 2017). PG was normalized in the *Synechocystis* sample by fixing its proportion at 25°C to previous quantifications used as a reference (Yuzawa et al. 2014).

**Figure Legends**

**Fig. 1. Incubation of cyanobacteria on the surface of gypsum polycrystalline chips in desiccation conditions.** (**A**) Pigmentation of cyanobacterial deposits on the surface of the chips over a 15 days period of incubation. (**B**) Comparison of the XRD chip profiles for 3 replicates of each strain after 15 days of incubation. (**C**) Comparison of the obtained chips XRD profiles after 15 days of incubation with the different strains with the standard profiles from the International Centre for Diffraction Data (ICDD) database, i.e. 01-080-6362 (β-anhydrite), 04-011-1764 (γ-anhydrite), 01-080-7957 (Bassanite), and 04-009-1810 (Gypsum). AU, arbitrary unit. θ = angle of diffraction.

**Fig. 2. Survival of cyanobacteria after desiccation on a gypsum surface.** The chlorophyll concentration was measured as a function of time in BG11 media after incubation of the inoculated chips with the two strains. The flasks were maintained at 25°C with 20 $\mu$mol photon.m$^{-2}$.s$^{-1}$ of light with orbital shaking. Graphs indicate the average of values obtained in triplicates. Error bars show standard deviations.

**Fig. 3. *Chroococcidiopsis* and *Synechocystis* maximum quantum efficiency (Fv/Fm).** The Fv/Fm values were obtained using the PSI Fluor pen FP110, following the OJIP protocol, after 5 min dark relaxation. (**A**) **Photosynthesis efficiency of cyanobacteria after desiccation on a gypsum surface.** Dehydrated gypsum chip samples were re-hydrated with sterile distilled water in the dark for 30 min prior the measure. (**B**) **Photosynthesis efficiency of cyanobacteria after cultivation at different temperatures.** Growth was performed in BG11 medium with 2 mM total inorganic carbon. The pH was kept constant at 7.5 by bubbling 3,000 ppm $CO_2$ mixed with air at 100 mL.min$^{-1}$ in a Multicultivator at the indicated temperature. The light was set constant at 20 $\mu$mol photon.m$^{-2}$.s$^{-1}$. G, *Chroococcidiopsis* G-MTQ-3P2; Syn, *Synechocystis* PCC 6803.

**Fig. 4. Comparison of the ultrastructure of the two cyanobacterial strains *Synechocystis* PCC 6803 (A, B) and *Chroococcidiopsis* G-MTQ-3P2 (C, D) in liquid culture and after 21 days of drying onto a gypsum chip.** Image parameters: A, bar 300 nm, working distance (WD) 4.6 mm, magnification (mag) 43,730x; B, bar 300 nm, WD 4.7 mm, mag 52,440 x; C, bar 400 nm, WD 4.6mm, mag 37,210 x; D, bar 400 nm, WD 4.6 mm, mag 32,440 x. The arrows indicate thylakoidal membranes.

**Fig. 5. Relative proportions of the major lipid classes upon change of growth conditions. Effect of (A) desiccation and (B) growth temperature on the membrane lipid profiles of *Synechocystis* and *Chroococcidiopsis*.** Relative proportions of the four major membrane lipid classes were evaluated as described in methods. Values correspond to the average obtained from triplicates. Error bars correspond to standard deviation. Monogalactosyldiacylglycerol, MGDG; diagalactosyldiacylglycerol, DGDG; sulfoquinovosyldiacylglycerol, SQDG; phosphatidylglycerol, PG.

**Fig. 6. Remodeling of acyl profiles of each membrane lipid class in *Synechocystis* and *Chroococcidiopsis* exposed to desiccation. (A)** MGDG, **(B)** DGDG, **(C)** SQDG and **(D)** PG acyl profiles as a function of the dehydration progression, up to 21 days. Values correspond to the average obtained from triplicates. Error bars correspond to standard deviation.

**Fig. 7. Remodeling of acyl profiles of each membrane lipid class in *Synechocystis* and *Chroococcidiopsis* exposed to desiccation. (A)** MGDG, **(B)** DGDG, **(C)** SQDG and **(D)** PG acyl profiles as a function of growth temperature. Values correspond to the average obtained from triplicates. Error bars correspond to standard deviation.

**Fig. 8. Analysis of low temperature fluorescence emission spectra upon excitation of the phycobilisomes at 572 nm.** (**A**) and (**B**) show the effect of temperature adaptation on the low temperature excitation profile comparing *Synechocystis* and *Chroococcidiopsis*, respectively. The curves represent relative intensities, and were normalized by superimposing the value at 695 nm (PSII peak). (**C**) and (**D**) show the effect of dehydration on the same profile on *Synechocystis* and *Chroococcidiopsis*, respectively. The curves represent relative intensities, and were normalized by superimposing the phycobilisome peak, avoiding a normalization on PSII peak, as this peak disappears in *Synechocystis* after three weeks of desiccation. Curves are the average of three normalized biological replicates.

**References**

Abida, H., Dolch, L.J., Mei, C., Villanova, V., Conte, M., Block, M.A., et al. (2015) Membrane glycerolipid remodeling triggered by nitrogen and phosphorus starvation in Phaeodactylum tricornutum. *Plant Physiol* 167: 118-136.

Aoki, M., Sato, N., Meguro, A. and Tsuzuki, M. (2004) Differing involvement of sulfoquinovosyl diacylglycerol in photosystem II in two species of unicellular cyanobacteria. *Eur J Biochem* 271: 685-693.

Apdila, E.T. and Awai, K. (2018) Configuration of the sugar head of glycolipids in thylakoid membranes. *Genes Genet Syst* 92: 235-242.

Bahl, J., Lau, M.C.Y., Smith, G.J.D., Vijaykrishna, D., Cary, S.C., Lacap, D.C., et al. (2011) Ancient origins determine global biogeography of hot and cold desert cyanobacteria. *Nature Communications* 2.

Baldanta, S., Arnal, R., Blanco-Rivero, A., Guevara, G. and Navarro Llorens, J.M. (2023) First characterization of cultivable extremophile Chroococcidiopsis isolates from a solar panel. *Frontiers in microbiology* 14: 982422.

Baque, M., Viaggiu, E., Scalzi, G. and Billi, D. (2013) Endurance of the endolithic desert cyanobacterium Chroococcidiopsis under UVC radiation. *Extremophiles* 17: 161-169.

Billi, D., Blanco, Y., Ianneo, A., Moreno-Paz, M., Aguirre, J., Baque, M., et al. (2022) Mars-like UV Flux and Ionizing Radiation Differently Affect Biomarker Detectability in the Desert Cyanobacterium Chroococcidiopsis as Revealed by the Life Detector Chip Antibody Microarray. *Astrobiology* 22: 1199-1209.

Billi, D., Friedmann, E.I., Helm, R.F. and Potts, M. (2001) Gene transfer to the desiccation-tolerant cyanobacterium Chroococcidiopsis. *J Bacteriol* 183: 2298-2305.

Billi, D., Friedmann, E.I., Hofer, K.G., Caiola, M.G. and Ocampo-Friedmann, R. (2000) Ionizing-radiation resistance in the desiccation-tolerant cyanobacterium Chroococcidiopsis. *Appl Environ Microbiol* 66: 1489-1492.

Billi, D., Verseux, C., Fagliarone, C., Napoli, A., Baque, M. and de Vera, J.P. (2019) A Desert Cyanobacterium under Simulated Mars-like Conditions in Low Earth Orbit: Implications for the Habitability of Mars. *Astrobiology* 19: 158-169.

Bligh, G.E. and Dyer, W.J. (1959) A rapid method of total lipid extraction and purification. *Can. J. Biochem. Physiol.* 37: 911-917.

Bolik, S., Albrieux, C., Schneck, E., Deme, B. and Jouhet, J. (2022) Sulfoquinovosyldiacylglycerol and phosphatidylglycerol bilayers share biophysical properties and are good mutual substitutes in photosynthetic membranes. *Biochim Biophys Acta Biomembr* 1864: 184037.

Bolte, K., Kawach, O., Prechtl, J., Gruenheit, N., Nyalwidhe, J. and Maier, U.G. (2008) Complementation of a phycocyanin-bilin lyase from Synechocystis sp. PCC 6803 with a nucleomorph-encoded open reading frame from the cryptophyte Guillardia theta. *BMC Plant Biol* 8: 56.

Boudiere, L., Michaud, M., Petroutsos, D., Rebeille, F., Falconet, D., Bastien, O., et al. (2014) Glycerolipids in photosynthesis: composition, synthesis and trafficking. *Biochim Biophys Acta* 1837: 470-480.

Brody, S.S. (1958) New Excited State of Chlorophyll. *Science* 128: 838-839.

Camara, B., Suzuki, S., Nealson, K.H., Wierzchos, J., Ascaso, C., Artieda, O., et al. (2014) Ignimbrite textural properties as determinants of endolithic colonization patterns from hyper-arid Atacama Desert. *Int Microbiol* 17: 235-247.

Campbell, D. and Oquist, G. (1996) Predicting Light Acclimation in Cyanobacteria from Nonphotochemical Quenching of Photosystem II Fluorescence, Which Reflects State Transitions in These Organisms. *Plant Physiol* 111: 1293-1298.

Capuano, V., Braux, A.S., Tandeau de Marsac, N. and Houmard, J. (1991) The "anchor polypeptide" of cyanobacterial phycobilisomes. Molecular characterization of the Synechococcus sp. PCC 6301 apce gene. *J Biol Chem* 266: 7239-7247.

Casero, M.C., Ascaso, C., Quesada, A., Mazur-Marzec, H. and Wierzchos, J. (2021) Response of Endolithic Chroococcidiopsis Strains From the Polyextreme Atacama Desert to Light Radiation. *Frontiers in microbiology* 11: 614875.

Chitnis, V.P. and Chitnis, P.R. (1993) PsaL subunit is required for the formation of photosystem I trimers in the cyanobacterium Synechocystis sp. PCC 6803. *FEBS Lett* 336: 330-334.

Cockell, C.S., Schuerger, A.C., Billi, D., Friedmann, E.I. and Panitz, C. (2005) Effects of a simulated martian UV flux on the cyanobacterium, Chroococcidiopsis sp. 029. *Astrobiology* 5: 127-140.

Coleine, C., Stajich, J.E., de Los Rios, A. and Selbmann, L. (2021) Beyond the extremes: Rocks as ultimate refuge for fungi in drylands. *Mycologia* 113: 108-133.

de Alvarenga, L.V., Lucius, S., Vaz, M., Araujo, W.L. and Hagemann, M. (2020) The novel strain Desmonostoc salinum CCM-UFV059 shows higher salt and desiccation resistance compared to the model strain Nostoc sp. PCC7120. *J Phycol* 56: 496-506.

Dobson, Z., Ahad, S., Vanlandingham, J., Toporik, H., Vaughn, N., Vaughn, M., et al. (2021) The structure of photosystem I from a high-light-tolerant cyanobacteria. *Elife* 10.

Elanskaya, I.V., Zlenko, D.V., Lukashev, E.P., Suzina, N.E., Kononova, I.A. and Stadnichuk, I.N. (2018) Phycobilisomes from the mutant cyanobacterium Synechocystis sp. PCC 6803 missing chromophore domain of ApcE. *Biochim Biophys Acta Bioenerg* 1859: 280-291.

Fardelli, E., D'Arco, A., Lupi, S., Billi, D., Moeller, R. and Guidi, M.C. (2023) Spectroscopic evidence of the radioresistance of Chroococcidiopsis biosignatures: A combined Raman, FT-IR and THz-TDs spectroscopy study. *Spectrochim Acta A Mol Biomol Spectrosc* 288: 122148.

Flori, S., Jouneau, P.H., Gallet, B., Estrozi, L.F., Moriscot, C., Schoehn, G., et al. (2018) Imaging Plastids in 2D and 3D: Confocal and Electron Microscopy. *Methods Mol Biol* 1829: 113-122.

Frentzen, M. (2004) Phosphatidylglycerol and sulfoquinovosyldiacylglycerol: anionic membrane lipids and phosphate regulation. *Current Opinion in Plant Biology* 7: 270-276.

Friedmann, E.I. and Ocampo-Friedmann, R. (1995) A primitive cyanobacterium as pioneer microorganism for terraforming Mars. *Adv Space Res* 15: 243-246.

Gomez-Silva, B. (2018) Lithobiontic life: "Atacama rocks are well and alive". *Anton Leeuw Int J G* 111: 1333-1343.

Gomez-Silva, B., Vilo-Munoz, C., Galetovic, A., Dong, Q.F., Castelan-Sanchez, H.G., Perez-Llano, Y., et al. (2019) Metagenomics of Atacama Lithobiontic Extremophile Life Unveils Highlights on Fungal Communities, Biogeochemical Cycles and Carbohydrate-Active Enzymes. *Microorganisms* 7.

Grunzweig, J.M., De Boeck, H.J., Rey, A., Santos, M.J., Adam, O., Bahn, M., et al. (2022) Dryland mechanisms could widely control ecosystem functioning in a drier and warmer world. *Nat Ecol Evol* 6: 1064-1076.

Gueguen, N. and Marechal, E. (2021) Origin of Cyanobacterial thylakoids via a non-vesicular glycolipid phase transition and impact on the Great Oxygenation Event. *J Exp Bot*.

Guler, S., Seeliger, A., Hartel, H., Renger, G. and Benning, C. (1996) A null mutant of Synechococcus sp PCC7942 deficient in the sulfolipid sulfoquinovosyl diacylglycerol. *Journal of Biological Chemistry* 271: 7501-7507.

Hagemann, M., Henneberg, M., Felde, V.J., Drahorad, S.L., Berkowicz, S.M., Felix-Henningsen, P., et al. (2015) Cyanobacterial Diversity in Biological Soil Crusts along a Precipitation Gradient, Northwest Negev Desert, Israel. *Microb Ecol* 70: 219-230.

Hewelt-Belka, W., Kot-Wasik, A., Tamagnini, P. and Oliveira, P. (2020) Untargeted Lipidomics Analysis of the Cyanobacterium Synechocystis sp. PCC 6803: Lipid Composition Variation in Response to Alternative Cultivation Setups and to Gene Deletion. *International journal of molecular sciences* 21.

Huang, W., Ertekin, E., Wang, T., Cruz, L., Dailey, M., DiRuggiero, J., et al. (2020) Mechanism of water extraction from gypsum rock by desert colonizing microorganisms. *Proc Natl Acad Sci U S A* 117: 10681-10687.

Jahns, P. and Holzwarth, A.R. (2012) The role of the xanthophyll cycle and of lutein in photoprotection of photosystem II. *Biochim Biophys Acta* 1817: 182-193.

Jordan, P., Fromme, P., Witt, H.T., Klukas, O., Saenger, W. and Krauss, N. (2001) Three-dimensional structure of cyanobacterial photosystem I at 2.5 A resolution. *Nature* 411: 909-917.

Jouhet, J. (2013) Importance of the hexagonal lipid phase in biological membrane organization. *Frontiers in plant science* 4: 494.

Jouhet, J., Lupette, J., Clerc, O., Magneschi, L., Bedhomme, M., Collin, S., et al. (2017) LC-MS/MS versus TLC plus GC methods: Consistency of glycerolipid and fatty acid profiles in microalgae and higher plant cells and effect of a nitrogen starvation. *PLOS ONE* 12: e0182423.

Kilian, O., Steunou, A.S., Fazeli, F., Bailey, S., Bhaya, D. and Grossman, A.R. (2007) Responses of a thermophilic Synechococcus isolate from the microbial mat of octopus spring to light. *Appl Environ Microb* 73: 4268-4278.

Kirilovsky, D. and Wilson, A. (2007) A new photoactive protein acting as a sensor of light intensity: the Orange Carotenoid Protein (OCP). *Photosynthesis Research* 91: 291-292.

Klodawska, K., Bujas, A., Turos-Cabal, M., Zbik, P., Fu, P. and Malec, P. (2019) Effect of growth temperature on biosynthesis and accumulation of carotenoids in cyanobacterium Anabaena sp. PCC 7120 under diazotrophic conditions. *Microbiol Res* 226: 34-40.

Komatsu, H., Wada, K., Kanjoh, T., Miyashita, H., Sato, M., Kawachi, M., et al. (2016) Unique chlorophylls in picoplankton Prochlorococcus sp. "Physicochemical properties of divinyl chlorophylls, and the discovery of monovinyl chlorophyll b as well as divinyl chlorophyll b in the species Prochlorococcus NIES-2086". *Photosynth Res* 130: 445-467.

Kosourov, S., Murukesan, G., Jokela, J. and Allahverdiyeva, Y. (2016) Carotenoid Biosynthesis in Calothrix sp. 336/3: Composition of Carotenoids on Full Medium, During Diazotrophic Growth and After Long-Term H2 Photoproduction. *Plant Cell Physiol* 57: 2269-2282.

Kouril, R., Arteni, A.A., Lax, J., Yeremenko, N., D'Haene, S., Rogner, M., et al. (2005) Structure and functional role of supercomplexes of IsiA and Photosystem I in cyanobacterial photosynthesis. *FEBS Lett* 579: 3253-3257.

Lacap-Bugler, D.C., Lee, K.K., Archer, S., Gillman, L.N., Lau, M.C.Y., Leuzinger, S., et al. (2017) Global Diversity of Desert Hypolithic Cyanobacteria. *Frontiers in microbiology* 8: 867.

Laczko-Dobos, H. and Szalontai, B. (2009) Lipids, proteins, and their interplay in the dynamics of temperature-stressed membranes of a cyanobacterium, Synechocystis PCC 6803. *Biochemistry* 48: 10120-10128.

Lamb, J.J., Rokke, G. and Hohmann-Marriott, M.F. (2018) Chlorophyll fluorescence emission spectroscopy of oxygenic organisms at 77 K. *Photosynthetica* 56: 105-124.

Leverenz, R.L., Sutter, M., Wilson, A., Gupta, S., Thurotte, A., Bourcier de Carbon, C., et al. (2015) PHOTOSYNTHESIS. A 12 A carotenoid translocation in a photoswitch associated with cyanobacterial photoprotection. *Science* 348: 1463-1466.

Li, C., Zhang, X., Ye, T., Li, X. and Wang, G. (2022) Protection and Damage Repair Mechanisms Contributed To the Survival of Chroococcidiopsis sp. Exposed To a Mars-Like Near Space Environment. *Microbiol Spectr* 10: e0344022.

Li, M., Semchonok, D.A., Boekema, E.J. and Bruce, B.D. (2014) Characterization and evolution of tetrameric photosystem I from the thermophilic cyanobacterium Chroococcidiopsis sp TS-821. *Plant Cell* 26: 1230-1245.

Li, Y.Y., Chen, X.H., Xue, C., Zhang, H., Sun, G., Xie, Z.X., et al. (2019) Proteomic Response to Rising Temperature in the Marine Cyanobacterium Synechococcus Grown in Different Nitrogen Sources. *Frontiers in microbiology* 10: 1976.

Lichtenthaler, H.K. and Wellburn, A.R. (1983) Determinations of total carotenoids and chlorophylls a and b of leaf extracts in different solvents. *Biochem Soc Trans* 11: 591-592.

Liu, X.G., Xu, H., Zhang, J.Y., Liang, G.W., Liu, Y.T. and Guo, A.G. (2012) Effect of low temperature on chlorophyll biosynthesis in albinism line of wheat (Triticum aestivum) FA85. *Physiol Plant* 145: 384-394.

Mavroudakis, L., Valsami, E.A., Grafanaki, S., Andreadaki, T.P., Ghanotakis, D.F. and Pergantis, S.A. (2019) The effect of nitrogen starvation on membrane lipids of Synechocystis sp. PCC 6803 investigated by using easy ambient sonic-spray ionization mass spectrometry. *Biochim Biophys Acta Biomembr* 1861: 183027.

Michel, K.P. and Pistorius, E.K. (2004) Adaptation of the photosynthetic electron transport chain in cyanobacteria to iron deficiency: The function of IdiA and IsiA. *Physiol Plant* 120: 36-50.

Mochimaru, M., Masukawa, H., Maoka, T., Mohamed, H.E., Vermaas, W.F. and Takaichi, S. (2008) Substrate specificities and availability of fucosyltransferase and beta-carotene hydroxylase for myxol 2'-fucoside synthesis in Anabaena sp. strain PCC 7120 compared with Synechocystis sp. strain PCC 6803. *J Bacteriol* 190: 6726-6733.

Mohamed, H.E., van de Meene, A.M., Roberson, R.W. and Vermaas, W.F. (2005) Myxoxanthophyll is required for normal cell wall structure and thylakoid organization in the cyanobacterium Synechocystis sp. strain PCC 6803. *J Bacteriol* 187: 6883-6892.

Mullineaux, P.M., Exposito-Rodriguez, M., Laissue, P.P. and Smirnoff, N. (2018) ROS-dependent signalling pathways in plants and algae exposed to high light: Comparisons with other eukaryotes. *Free Radic Biol Med*.

Murata, N., Nishimura, M. and Takamiya, A. (1966) Fluorescence of chlorophyll in photosynthetic systems. 3. Emission and action spectra of fluorescence--three emission bands of chlorophyll a and the energy transfer between two pigment systems. *Biochim Biophys Acta* 126: 234-243.

Murray, B., Dailey, M., Ertekin, E. and DiRuggiero, J. (2021) Draft Metagenomes of Endolithic Cyanobacteria and Cohabitants from Hyper-Arid Deserts. *Microbiol Resour Announc* 10: e0020621.

Murray, B., Ertekin, E., Dailey, M., Soulier, N.T., Shen, G., Bryant, D.A., et al. (2022) Adaptation of Cyanobacteria to the Endolithic Light Spectrum in Hyper-Arid Deserts. *Microorganisms* 10.

Nurnberg, D.J., Morton, J., Santabarbara, S., Telfer, A., Joliot, P., Antonaru, L.A., et al. (2018) Photochemistry beyond the red limit in chlorophyll f-containing photosystems. *Science* 360: 1210-1213.

Ogawa, T., Harada, T., Ozaki, H. and Sonoike, K. (2013) Disruption of the ndhF1 gene affects Chl fluorescence through state transition in the Cyanobacterium Synechocystis sp. PCC 6803, resulting in apparent high efficiency of photosynthesis. *Plant Cell Physiol* 54: 1164-1171.

Okanenko, A., Taran, N. and Kosyk, O. (2003) Sulphoquinovosyldiacylglycerol and adaptation syndrome. *Advanced Research on Plant Lipids*: 361-364.

Ossenbuhl, F., Inaba-Sulpice, M., Meurer, J., Soll, J. and Eichacker, L.A. (2006) The Synechocystis sp PCC 6803 oxa1 homolog is essential for membrane integration of reaction center precursor protein pD1. *Plant Cell* 18: 2236-2246.

Pittera, J., Jouhet, J., Breton, S., Garczarek, L., Partensky, F., Marechal, E., et al. (2018) Thermoacclimation and genome adaptation of the membrane lipidome in marine Synechococcus. *Environmental microbiology* 20: 612-631.

Plohnke, N., Seidel, T., Kahmann, U., Rogner, M., Schneider, D. and Rexroth, S. (2015) The proteome and lipidome of Synechocystis sp. PCC 6803 cells grown under light-activated heterotrophic conditions. *Mol Cell Proteomics* 14: 572-584.

Proctor, M.S., Pazdernik, M., Jackson, P.J., Pilny, J., Martin, E.C., Dickman, M.J., et al. (2020) Xanthophyll carotenoids stabilise the association of cyanobacterial chlorophyll synthase with the LHC-like protein HliD. *Biochem J* 477: 4021-4036.

Raanan, H., Oren, N., Treves, H., Keren, N., Ohad, I., Berkowicz, S.M., et al. (2016) Towards clarifying what distinguishes cyanobacteria able to resurrect after desiccation from those that cannot: The photosynthetic aspect. *Biochim Biophys Acta* 1857: 715-722.

Renger, G. (2007) Primary Processes of Photosynthesis, Part 1 Principles and Apparatus. *Compr Ser Photoch* 8: Vii-Ix.

Rzymski, P., Poniedzialek, B., Hippmann, N. and Kaczmarek, L. (2022) Screening the Survival of Cyanobacteria Under Perchlorate Stress. Potential Implications for Mars In Situ Resource Utilization. *Astrobiology* 22: 672-684.

Sato, N. and Awai, K. (2016) Diversity in Biosynthetic Pathways of Galactolipids in the Light of Endosymbiotic Origin of Chloroplasts. *Frontiers in plant science* 7.

Sato, N., Kamimura, R. and Tsuzuki, M. (2016) Dispensability of a sulfolipid for photoautotrophic cell growth and photosynthesis in a marine cyanobacterium, Synechococcus sp. PCC 7002. *Biochem Biophys Res Commun* 477: 854-860.

Sauer, J., Schreiber, U., Schmid, R., Volker, U. and Forchhammer, K. (2001) Nitrogen starvation-induced chlorosis in Synechococcus PCC 7942. Low-level photosynthesis as a mechanism of long-term survival. *Plant Physiol* 126: 233-243.

Schneegurt, M.A., Sherman, D.M., Nayar, S. and Sherman, L.A. (1994) Oscillating behavior of carbohydrate granule formation and dinitrogen fixation in the cyanobacterium Cyanothece sp. strain ATCC 51142. *J Bacteriol* 176: 1586-1597.

Semchonok, D.A., Mondal, J., Cooper, C.J., Schlum, K., Li, M., Amin, M., et al. (2022) Cryo-EM structure of a tetrameric photosystem I from Chroococcidiopsis TS-821, a thermophilic, unicellular, non-heterocyst-forming cyanobacterium. *Plant Commun* 3: 100248.

Shen, G.Z. and Vermaas, W.F.J. (1994) Chlorophyll in a Synechocystis Sp Pcc-6803 Mutant without Photosystem-I and Photosystem-Ii Core Complexes - Evidence for Peripheral Antenna Chlorophylls in Cyanobacteria. *Journal of Biological Chemistry* 269: 13904-13910.

Shimojima, M. (2011) Biosynthesis and functions of the plant sulfolipid. *Prog Lipid Res* 50: 234-239.

Simionato, D., Sforza, E., Corteggiani Carpinelli, E., Bertucco, A., Giacometti, G.M. and Morosinotto, T. (2011) Acclimation of Nannochloropsis gaditana to different illumination regimes: effects on lipids accumulation. *Bioresour Technol* 102: 6026-6032.

Sobotka, R., Duhring, U., Komenda, J., Peter, E., Gardian, Z., Tichy, M., et al. (2008) Importance of the cyanobacterial Gun4 protein for chlorophyll metabolism and assembly of photosynthetic complexes. *J Biol Chem* 283: 25794-25802.

Spat, P., Klotz, A., Rexroth, S., Macek, B. and Forchhammer, K. (2018) Chlorosis as a Developmental Program in Cyanobacteria: The Proteomic Fundament for Survival and Awakening. *Mol Cell Proteomics* 17: 1650-1669.

Strasser, R.J., Srivastava, A. and Tsimilli-Michael, M. (2000) The fluorescence transient as a tool to characterize and screen photosynthetic samples. In *Probing photosynthesis: mechanisms, regulation and adaptation*. Edited by Yunus, M., Pathre, U. and Mohanty, P. pp. 445-483. CRC Press, Boca Raton, FL.

Tamaru, Y., Takani, Y., Yoshida, T. and Sakamoto, T. (2005) Crucial role of extracellular polysaccharides in desiccation and freezing tolerance in the terrestrial cyanobacterium Nostoc commune. *Appl Environ Microbiol* 71: 7327-7333.

Tamary, E., Kiss, V., Nevo, R., Adam, Z., Bernat, G., Rexroth, S., et al. (2012) Structural and functional alterations of cyanobacterial phycobilisomes induced by high-light stress. *Biochim Biophys Acta* 1817: 319-327.

Taniguchi, M. and Lindsey, J.S. (2021) Absorption and Fluorescence Spectral Database of Chlorophylls and Analogues. *Photochem Photobiol* 97: 136-165.

Taran, N., Okanenko, A. and Musienko, N. (2000) Sulpholipid reflects plant resistance to stress-factor action. *Biochemical Society Transactions* 28: 922-924.

Taranto, P.A., Keenan, T.W. and Potts, M. (1993) Rehydration induces rapid onset of lipid biosynthesis in desiccated Nostoc commune (Cyanobacteria). *Biochim Biophys Acta* 1168: 228-237.

Toporik, H., Li, J., Williams, D., Chiu, P.L. and Mazor, Y. (2019) The structure of the stress-induced photosystem I-IsiA antenna supercomplex. *Nat Struct Mol Biol* 26: 443-449.

van de Meene, A.M., Hohmann-Marriott, M.F., Vermaas, W.F. and Roberson, R.W. (2006) The three-dimensional structure of the cyanobacterium Synechocystis sp. PCC 6803. *Arch Microbiol* 184: 259-270.

Van Mooy, B.A., Rocap, G., Fredricks, H.F., Evans, C.T. and Devol, A.H. (2006) Sulfolipids dramatically decrease phosphorus demand by picocyanobacteria in oligotrophic marine environments. *Proc Natl Acad Sci U S A* 103: 8607-8612.

van Stokkum, I.H.M., Gwizdala, M., Tian, L., Snellenburg, J.J., van Grondelle, R., van Amerongen, H., et al. (2018) A functional compartment model of the Synechocystis PCC 6803 phycobilisome. *Photosynth Res* 135: 87-102.

Verseux, C., Baque, M., Cifariello, R., Fagliarone, C., Raguse, M., Moeller, R., et al. (2017) Evaluation of the Resistance of Chroococcidiopsis spp. to Sparsely and Densely Ionizing Irradiation. *Astrobiology* 17: 118-125.

Walker, J.J. and Pace, N.R. (2007) Endolithic microbial ecosystems. *Annu Rev Microbiol* 61: 331-347.

Wang, X., Yang, Z., Liu, Y., Wang, X., Zhang, H., Shang, R., et al. (2022) Structural characteristic of polysaccharide isolated from Nostoc commune, and their potential as radical scavenging and antidiabetic activities. *Scientific reports* 12: 22155.

Welkie, D.G., Sherman, D.M., Chrisler, W.B., Orr, G. and Sherman, L.A. (2013) Analysis of carbohydrate storage granules in the diazotrophic cyanobacterium Cyanothece sp. PCC 7822. *Photosynth Res* 118: 25-36.

Wierzchos, J., Artieda, O., Ascaso, C., Garcia, F.N., Vitek, P., Azua-Bustos, A., et al. (2020) Crystalline water in gypsum is unavailable for cyanobacteria in laboratory experiments and in natural desert endolithic habitats. *Proceedings of the National Academy of Sciences of the United States of America* 117: 27786-27787.

Wierzchos, J., Casero, M.C., Artieda, O. and Ascaso, C. (2018) Endolithic microbial habitats as refuges for life in polyextreme environment of the Atacama Desert. *Current Opinion in Microbiology* 43: 124-131.

Xiong, W., Shen, G. and Bryant, D.A. (2017) Synechocystis sp. PCC 6803 CruA (sll0147) encodes lycopene cyclase and requires bound chlorophyll a for activity. *Photosynth Res* 131: 267-280.

Yuzawa, Y., Shimojima, M., Sato, R., Mizusawa, N., Ikeda, K., Suzuki, M., et al. (2014) Cyanobacterial monogalactosyldiacylglycerol-synthesis pathway is involved in normal unsaturation of galactolipids and low-temperature adaptation of Synechocystis sp. PCC 6803. *Biochim Biophys Acta* 1841: 475-483.

Zhu, Y.H., Graham, J.E., Ludwig, M., Xiong, W., Alvey, R.M., Shen, G.Z., et al. (2010) Roles of xanthophyll carotenoids in protection against photoinhibition and oxidative stress in the cyanobacterium Synechococcus sp strain PCC 7002. *Archives of Biochemistry and Biophysics* 504: 86-99.
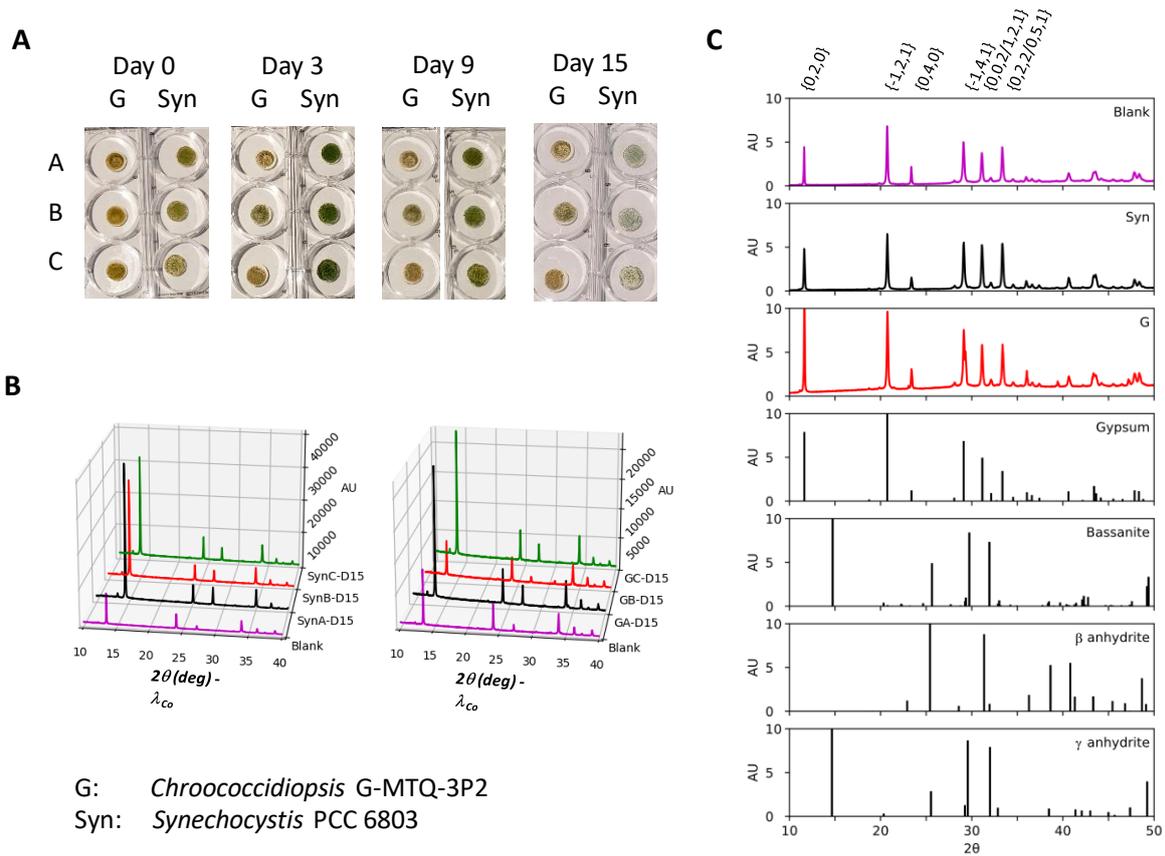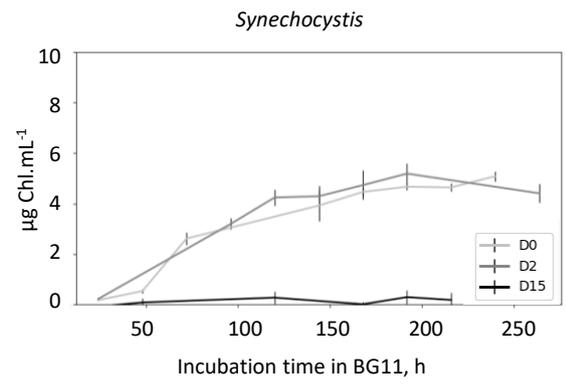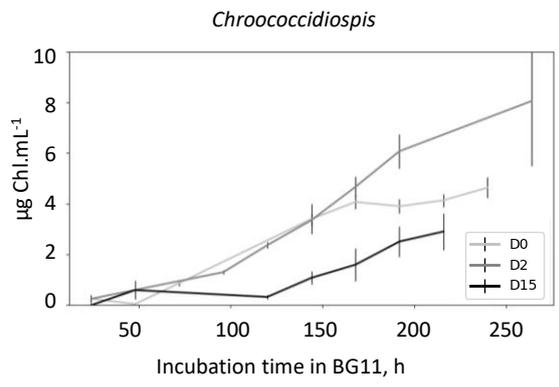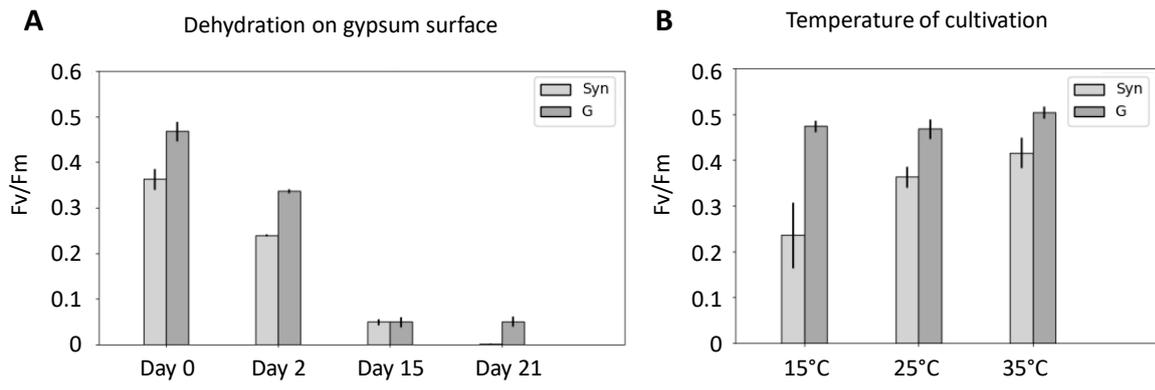
**A**

Day 0 | Day 3 | Day 9 | Day 15
G  Syn | G  Syn | G  Syn | G  Syn

A
B
C

**B**

SynC-D15
SynB-D15
SynA-D15
Blank

GC-D15
GB-D15
GA-D15
Blank

$2\theta(deg) - \lambda_{Co}$

$2\theta(deg) - \lambda_{Co}$

G:   *Chroococcidiopsis* G-MTQ-3P2
Syn:  *Synechocystis* PCC 6803

**C**

{0,2,0}  {-1,2,1}  {0,4,0}  {-1,4,1}  {0,0,2}/{1,2,1}  {0,2,2}/{0,5,1}

Blank
Syn
G
Gypsum
Bassanite
β anhydrite
γ anhydrite

$2\theta$

Fig 1

Fig 2

**A** Dehydration on gypsum surface

**B** Temperature of cultivation

Fig 3

*Synechocystis* PCC 6803
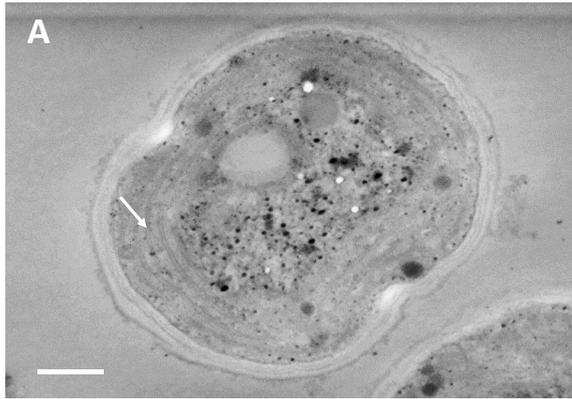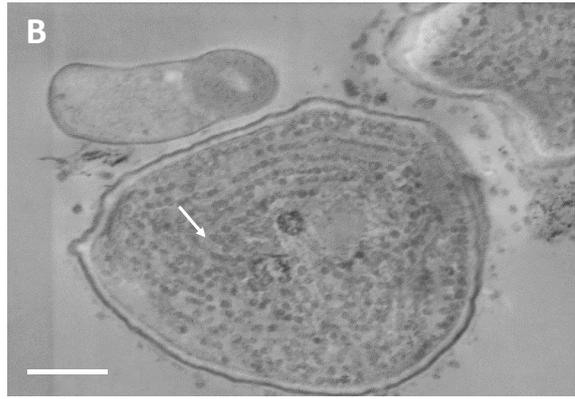
*Chroococcidiopsis* G-MTQ-3P2

Fig 4

Fig 5

Fig 6

Fig 7

Fig 8